THE JOURNAL OF COMPARATIVE NEUROLOGY 407:555–582 (1999)

Projections of the Median Raphe Nucleus in the Rat

ROBERT P. VERTES,[1]* WILLIAM J. FORTIN,[2] AND ALISON M. CRANE[3]
[1]Center for Complex Systems, Florida Atlantic University, Boca Raton, Florida 33431
[2]Department of Anatomy and Neurobiology, Dalhousie University,
Faculty of Medicine, Halifax, NS B3H 4H7, Canada
[3]Department of Psychology, University of Texas at Austin, Austin, Texas 78712

ABSTRACT

No previous report in any species has examined comprehensively the projections of the median raphe (MR) nucleus with modern tracing techniques. The present report represents an in depth analysis of the projections of MR by use of the anterograde anatomical tracer *Phaseolus vulgaris*-leucoagglutinin. MR fibers descend along the midline within the brainstem and mainly ascend within the medial forebrain bundle in the forebrain. MR fibers distribute densely to the following brainstem/forebrain sites: caudal raphe nuclei, laterodorsal tegmental nucleus, dorsal raphe nucleus, interpeduncular nucleus, medial mammillary body, supramammillary nucleus, posterior nucleus and perifornical region of the hypothalamus, midline and intralaminar nuclei of thalamus, dopamine-containing cell region of medial zona incerta, lateral habenula, horizontal and vertical limbs of the diagonal band nuclei, medial septum, and hippocampal formation. Virtually all of these structures lie on or close to the midline, indicating that the MR represents a midline/para-midline system of projections. Overall, MR projections to the cortex are light. MR projects moderately to the perirhinal, entorhinal and frontal cortices, but sparingly to remaining regions of cortex. A comparison of MR with dorsal raphe (DR) projections (Vertes RP. 1991. J Comp Neurol 313:643–668) shows that these two major serotonin-containing cell groups of the midbrain distribute to essentially nonoverlapping regions of the forebrain; that is, the MR and DR project to complementary sites in the forebrain. A direct role for the MR in the desynchronization of the electroencephalographic activity of the hippocampus and its possible consequences for memory-associated functions of the hippocampus is discussed. J. Comp. Neurol. 407:555–582, 1999.

Indexing terms: brainstem; supramammillary nucleus; lateral habenula; septum; hippocampus

The median raphe (MR) nucleus is a major serotonin-containing cell group of the brainstem (Steinbusch and Nieuwenhuys, 1983; Tork, 1985; Jacobs and Azmitia, 1992; Halliday et al., 1995; Vertes and Crane, 1997). A number of early reports, that used degeneration or autoradiographic techniques, examined MR projections in rats and cats (Conrad et al., 1974; Moore and Halaris, 1975; Bobillier et al., 1975, 1976, 1979; Moore et al., 1978; Azmitia and Segal, 1978). Although valuable early contributions, these reports essentially only described the main projection sites of MR fibers, not overall patterns of distribution. In addition, some early reports (Conrad et al., 1974; Moore et al., 1978) did not distinguish between the projections of the median and dorsal raphe nuclei (anterograde tracers spanned both cell groups), whereas other reports predominantly focused on MR projections to specific sites; that is, to the brainstem/diencephalon (Bobillier et al., 1975, 1976) or to the hippocampal formation (Moore and Halaris, 1975).

The most complete early analysis of MR projections was that of Azmitia and Segal (1978), which examined the differential ascending projections of the median and dorsal raphe (DR) nuclei in the rat by using the autoradiographic method. Although this study documented the various ascending routes taken by MR and DR fibers, it rather superficially described patterns of terminal distribution in target structures. Also, like previous studies, only major targets were examined. As part of a larger project analyzing the projections of the pontine and mesencephalic

Grant sponsor: NIH; Grant number: NS35883; Grant sponsor: NIMH; Grant number: MH10476.

*Correspondence to: Robert P. Vertes, Center for Complex Systems, Florida Atlantic University, Boca Raton, FL 33431.
E-mail: vertes@walt.ccs.fau.edu

Received 20 March 1998; Revised 15 December 1998; Accepted 21 December 1998

Abbreviations

AC	anterior commissure
ACC	nucleus accumbens
AD	anterodorsal nucleus of thalamus
AGl	agranular field of frontal cortex, lateral part
AGm	agranular field of frontal cortex, medial part
AH	anterior nucleus of hypothalamus
AM	anteromedial nucleus of thalamus
AMYG	amygdala
AO	anterior olfactory nucleus
APi	amygdalopiriform area
APN	anterior pretectal nucleus
AQ	aqueduct
AV	anteroventral nucleus of thalamus
BC	brachium conjunctivum
BCx	decussation of BC
BLA	basolateral nucleus of amygdala
BMA	basomedial nucleus of amygdala
BST/BNST	bed nucleus of stria terminalis
BP	brachium pontis
C	cerebellum
CB	cingulum bundle
CA1,3	CA1, CA3 fields of Ammon's horn
CC	corpus callosum
CEA	central nucleus of amygdala
CG	central gray
CgC	cingulate cortex
CL	central lateral nucleus of thalamus
CLA	claustrum
Cli	central linear nucleus of raphe
CM	central medial nucleus of thalamus
CN	cochlear nucleus
COAa	cortical nucleus of amygdala, anterior part
COAp	cortical nucleus of amygdala, posterior part
CP	cerebral peduncle
C-P	caudate-putamen
CUN	nucleus cuneiformis
DBh,v	horizontal, vertical limbs of diagonal band nuclei
DG	dentate gyrus of hippocampal formation
DGR	granule cell layer of dentate gyrus
DMh	dorsomedial nucleus of hypothalamus
DK	nucleus of Darkschewitsch
DR	dorsal raphe nucleus
DT	dorsal tegmental nucleus (of Gudden)
EC	entorhinal cortex
EN	endopiriform nucleus
F	fornix
FA	corpus callosum, anterior forceps
FI	fimbria of hippocampal formation
FL	forelimb area of cortex
FR	fasciculus retroflexus
FS	fundus of striatum
GP	globus pallidus
HC	hippocampal commissure
HF	hippocampal formation
HFi	hippocampal fissure
HL	hindlimb area of cortex
IC	inferior colliculus
ICa	internal capsule
ICP	inferior cerebellar peduncle
IL	infralimbic cortex
ILr	intralaminar nuclei of thalamus, rostral group
IMD	intermediodorsal nucleus of thalamus
InC	insular cortex
INC	nucleus incertus
IP	interpeduncular nucleus
IPr	interpeduncular nucleus, rostral subnucleus
LA	lateral nucleus of amygdala
LC	locus coeruleus
LD	laterodorsal nucleus of thalamus
LDT	laterodorsal tegmental nucleus
LGNd	lateral geniculate nucleus, dorsal division
LH	lateral habenula
LHy	lateral hypothalamus
LO	lateral olfactory tract
LP	lateroposterior nucleus of thalamus
LPB	lateral parabrachial nucleus
LPO	lateral preoptic area
LSd,i,v	lateral septum; dorsal, intermediate, ventral divisions
LV	lateral ventricle
MB	mammillary bodies
MD	mediodorsal nucleus of thalamus
MEA	medial nucleus of amygdala
MFB	medial forebrain bundle
MGN	medial geniculate nucleus
MgPO	magnocellular preoptic nucleus
MH	medial habenula
ML	medial lemniscus
mo	molecular layer of dentate gyrus
MO5	motor nucleus of trigeminal nerve
MPO	medial preoptic area
MR	median raphe nucleus
MRF	mesencephalic reticular formation
MS	medial septum
MT	mammillothalamic tract
MV	medial vestibular nucleus
N3	oculomotor nucleus
N6	abducens nucleus
N7	facial nucleus
NGC	nucleus gigantocellularis
NGCa	nucleus gigantocellularis, pars alpha
NLL	nucleus of lateral lemniscus
NP	nucleus of pons
OcC	occipital cortex
OT	optic tract
OX	optic chiasm
PaC	parietal cortex
PARA	parasubiculum
PC	paracentral nucleus of thalamus
PCo	posterior commissure
PF	parafascicular nucleus of thalamus
PFo	perifornical region of hypothalamus
PG	parabigeminal nucleus
PH	posterior nucleus of hypothalamus
PiC	piriform cortex
PL	prelimbic cortex
PMv	premammillary nucleus, ventral division
PN5	principal nucleus of trigeminal nerve
po	polymorphic layer of dentate gyrus
POST	postsubiculum
PPT	pedunculopontine tegmental nucleus
PrC	perirhinal cortex
PRE	presubiculum
PRF	pontine reticular formation
PrH	prepositus hypoglossal nucleus
PT	pyramidal tract
PV	paraventricular nucleus of thalamus
RE	nucleus reuniens of thalamus
RF	reticular formation
RH	rhomboid nucleus of thalamus
RM	raphe magnus
RN	red nucleus
RP	raphe pontis
RPC	nucleus pontis caudalis
RPO	nucleus pontis oralis
RR	retrorubral nucleus/area
RsC	retrosplenial cortex
RT	reticular nucleus of thalamus
RTG	reticular tegmental nucleus of pons
SC	superior colliculus
SCi,s	SC, intermediate and superficial layers
SF	septofimbrial nucleus
SH	septohippocampal nucleus
SI	substantia innominata
sl	stratum lucidum of hippocampus
slm	stratum lacunosum-moleculare of hippocampus
SM	stria medullaris
SME	nucleus submedius of thalamus
SN	substantia nigra
SNC	substantia nigra, pars compacta
SN5	spinal nucleus of trigeminal nerve
so	stratum oriens of hippocampus
SO	superior olive
sr	stratum radiatum of hippocampus
ST5	spinal trigeminal tract
SUB	subiculum
SUM	supramammillary nucleus
SV	superior vestibular nucleus
TB	trapezoid body
TeC	temporal cortex
VB	ventrobasal complex of thalamus

reticular formation, we (Vertes and Martin, 1988) examined the ascending projections of the MR to the diencephalon, basal forebrain, and hippocampal formation by using the autoradiographic technique. Although our report described projections to these regions, it also was incomplete in that certain areas of the brain were omitted, significantly, the brainstem and neocortex. In essence then, although several reports have examined MR projections, none have described them in their totality.

In addition, all previous examinations of MR projections used older, and at present not commonly used, anterograde tracing techniques (i.e., mainly autoradiography). The projections of MR have not been comprehensively analyzed in any species by using the *Phaseolus vulgaris*-leucoagglutinin (PHA-L) technique. The PHA-L technique offers several well-documented advantages over other anterograde tracing methods, including the ability (1) to make small, well-localized injections; (2) to identify specifically neurons incorporating the tracer; (3) to distinguish fibers of passage from terminal endings; and (4) to visualize entire axonal processes, including preterminal/terminal specializations (Gerfen and Sawchenko, 1984; Ter Horst et al., 1984).

Our interest in the projections of the median raphe nucleus stems from our findings that MR is directly involved in the desynchronization of the hippocampal EEG (for review, Vertes, 1986; Vertes and Kocsis, 1997). We showed early on that electrical stimulation of the MR desynchronized the hippocampal EEG (Vertes, 1981), and in a recent series of studies in rats that injections of pharmacologic agents into MR that inhibit the activity of serotonergic MR neurons generate theta (Vertes et al., 1994; Kinney et al., 1994, 1995). For instance, we demonstrated that injections of 5-hydroxytryptamine (5-HT) agonists (Vertes et al., 1994), excitatory amino acid antagonists (Kinney et al., 1994), or γ-aminobutyric acid (GABA) agonists (Kinney et al., 1995) into the MR but not into immediately surrounding regions of the brainstem (e.g., the dorsal raphe nucleus) generated theta at very short latencies (30–120 seconds) and for very long durations (45–90 minutes). Similar findings have recently been described in the behaving cat (Marrosu et al., 1996).

We comprehensively examined the projections of MR by using the PHA-L anterograde tracing technique. Among other findings, we demonstrated that the MR largely represents a midline system of connections; that is, MR fibers distribute heavily to midline structures of the brainstem and forebrain and, by contrast, minimally to structures removed from the midline, including most of the paleo/neocortex.

Abbreviations (continued)

VC	ventral cochlear nucleus
VL	ventrolateral nucleus of thalamus
VM	ventromedial nucleus of thalamus
VMh	ventromedial nucleus of hypothalamus
VP	ventral pallidum
VT	ventral tegmental nucleus (of Gudden)
VTA	ventral tegmental area
ZI	zona incerta
ZIm	zona incerta, rostromedial part
3V	third ventricle
4V	fourth ventricle
5	trigeminal nerve

MATERIALS AND METHODS

Single injections of PHA-L were made into the median raphe nucleus of 33 male Sprague-Dawley (Charles River, Wilmington, MA) rats, each weighing 275–325 g. These experiments were approved by the Florida Atlantic University Institutional Animal Care and Use Committee and conform to all Federal regulations and National Institutes of Health Guidelines for the care and use of laboratory animals.

Powdered lectin from PHA-L was reconstituted to 2.5% in 0.05 M sodium phosphate buffer, pH 7.4. The PHA-L solution was iontophoretically deposited in the brains of anesthetized rats by means of a glass micropipette with an outside tip diameter of 40–60 μM. Positive direct current (5–10 μA) was applied through a Grass stimulator (model 88) coupled with a high-voltage stimulator (Frederick Haer Co., Brunswick, ME) at two seconds "on"/two seconds "off" intervals for 30–40 minutes. After a survival time of 7–10 days, animals were deeply anesthetized with sodium pentobarbital and perfused transcardially with a buffered saline wash (pH 7.4, 300 ml/animal) followed by fixative (2.5% paraformaldehyde, 0.2–0.5% glutaraldehyde in 0.05 M phosphate buffer, pH 7.4) (300–500 ml/animal) and then by 10% sucrose in the same phosphate buffer (150 ml/animal). The brains were removed and stored overnight at 4°C in 20% sucrose in the same phosphate buffer. On the following day, 50-μm frozen sections were collected in phosphate-buffered saline (PBS, 0.9% sodium chloride in 0.01 M sodium phosphate buffer, pH 7.4) and incubated for 1 hour in diluent [10% normal rabbit serum (Colorado Serum, Denver, CO) and 1% Triton X-100 (Sigma Chemicals, St. Louis, MO), in PBS]. Sections were then incubated overnight (14–17 hours) at 4°C in primary antiserum directed against PHA-L (biotinylated goat anti–PHA-L, Vector Labs, Burlingame, CA) at a dilution of 1:500 in diluent. The next day, sections were washed five times for five minutes each (5 × 5 minutes) in PBS, and then incubated in the second antiserum (rabbit anti-sheep IgG, Pel-Freez, Rogers, AK) at a dilution of 1:500 in diluent for two hours. Sections were rinsed again (5 × 5 minutes) and incubated with peroxidase-antiperoxidase (goat origin, Sternberger Monoclonals, Baltimore, MD) at a dilution of 1:250 for two hours. The last two incubations were repeated (double-bridge procedure), with 5 × 5 minutes rinses after each incubation, for 1 hour each. After 5 × 5 minutes rinses, the sections were incubated in 0.05% 3,3′-diaminobenzidine (DAB) in PBS for 10 minutes, followed by a second 5-min DAB (same concentration) incubation to which 0.018% H_2O_2 had been added. Sections were then rinsed again in PBS (3 × 1 minutes) and mounted onto chrome-alum gelatin-coated slides. An adjacent series of sections from each rat was stained with cresyl violet for anatomical reference.

Sections were examined by using light and darkfield optics. PHA-L labeled cells (at injection sites) and fibers were plotted onto maps constructed from adjacent Nissl-stained sections. The main criteria used to distinguish labeled terminals from fibers of passage were (1) the presence or essential absence of axon/terminal specializations, and (2) the degree of axonal branching. Terminal sites were typically characterized by a dense array of highly branched axons containing numerous specializations (varicosities, terminal boutons), whereas passing fibers exhibited minimal branching and contained few

specializations. Representative samples of material judged particularly useful for emphasizing and/or clarifying points of text were illustrated with photomicrographs.

RESULTS

Two of thirty-three cases are schematically illustrated and described in detail; the total pattern of labeling in the brainstem/forebrain for case C606, and the pattern of labeling in the septum and hippocampus for case F14. Figure 1 depicts two levels of the injection site for case C606. Figures 2 and 3 show injection sites for each of the 33 cases. As shown, the injections vary in size and as a group the 33 injections span the entire caudorostral extent of MR. The labeling produced by the two schematically illustrated cases is representative of that found with the nonillustrated cases. Patterns of labeling were very consistent across cases. The main difference among cases was relative density of labeling; that is, light to moderate with small injections or dense with large injections.

Case C606: Ascending projections

Figure 4 schematically depicts the distribution of labeled fibers in the rostral pons, midbrain, and forebrain (i.e., rostral to MR) produced by a PHA-L injection in a mid-rostrocaudal part of MR (case C606). In all cases (as shown for case C606) in which injections were centered mediolaterally in MR, labeling was bilaterally symmetrical throughout the brain.

Patterns of subcortical labeling

Labeled fibers dispersed in several directions from the site of injection (Fig. 4A): dorsally, to the pontine central gray (CG), dorsolaterally to the dorsolateral pontine tegmentum, and laterally to the pontine reticular formation (PRF). Main terminal sites were the dorsal raphe nucleus (DR) and ventromedial regions of the CG, dorsally; the ventral half of the cuneiform nucleus (CUN) and the ventrally adjacent pendunculopontine tegmental area (PPT), dorsolaterally; and the medial one-third of nucleus pontis oralis (RPO), lateral to the injection. Mid-to-lateral regions of RPO were lightly to moderately labeled.

At the caudal midbrain (Fig. 4B,C), the majority of labeled fibers ascended on the lateral borders of the MR (Fig. 4B) and further rostrally, lateral to the central linear nucleus (Cli) (Fig. 4C). Labeled axons distributed (1) densely to the lateral wings of DR and to the interpeduncular nucleus; (2) moderately to the central midbrain tegmentum (mainly comprising the mesencephalic reticular formation) (MRF); and (3) lightly to the medial DR, ventromedial CG, central linear nucleus, and retrorubral nucleus (RR). The compact patch of labeled fibers lying between RR and the cerebral peduncle (heavier on the left) (Fig. 4C) appeared bound for the substantia nigra-pars compacta (SNC) (Fig. 4E,F).

At the rostral midbrain (Fig. 4D,E), the labeled fibers that caudally coursed lateral to the MR/CLi progressively turned ventrally, spread mediolaterally across the ventral tegmentum and ascended dorsal to the IP (Fig. 4D) and rostrally on the ventral surface of the brain around the fasciculus retroflexus (FR)(Fig. 4E). With the exception of terminal labeling within the ventral tegmental area (VTA) and DR (Fig. 5A) as well as light labeling in the SNC, CLi, CG, and the adjacent dorsal tegmentum, labeled axons

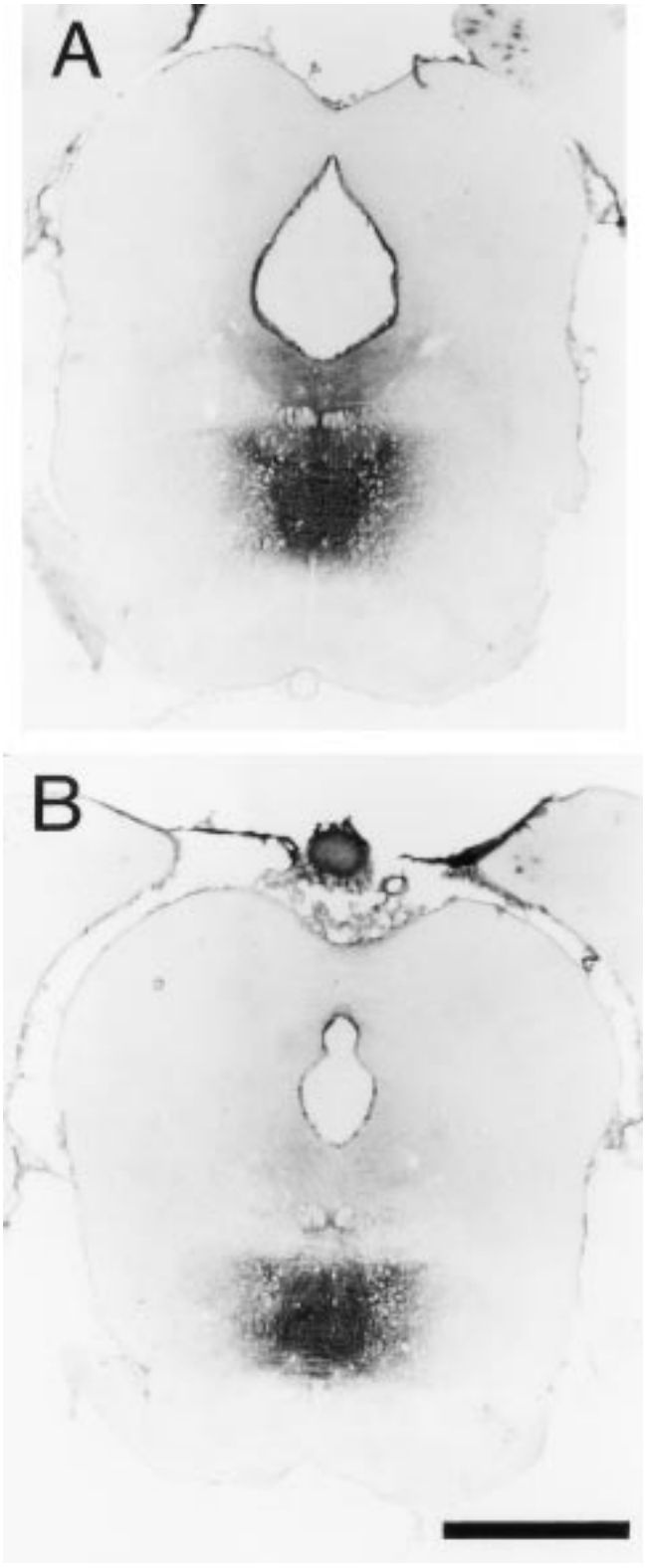

Fig. 1. Low-magnification lightfield photomicrographs showing the location of a *Phaseolus vulgaris*-leucoagglutinin injection in the median raphe nucleus for case C606 (**A**, caudal; **B**, rostral). Note the dispersion of labeled fibers from the sites of injection, medially to the pontine reticular formation and dorsally to the pontine central gray. Scale bar = 2 mm in B (applies to A,B).

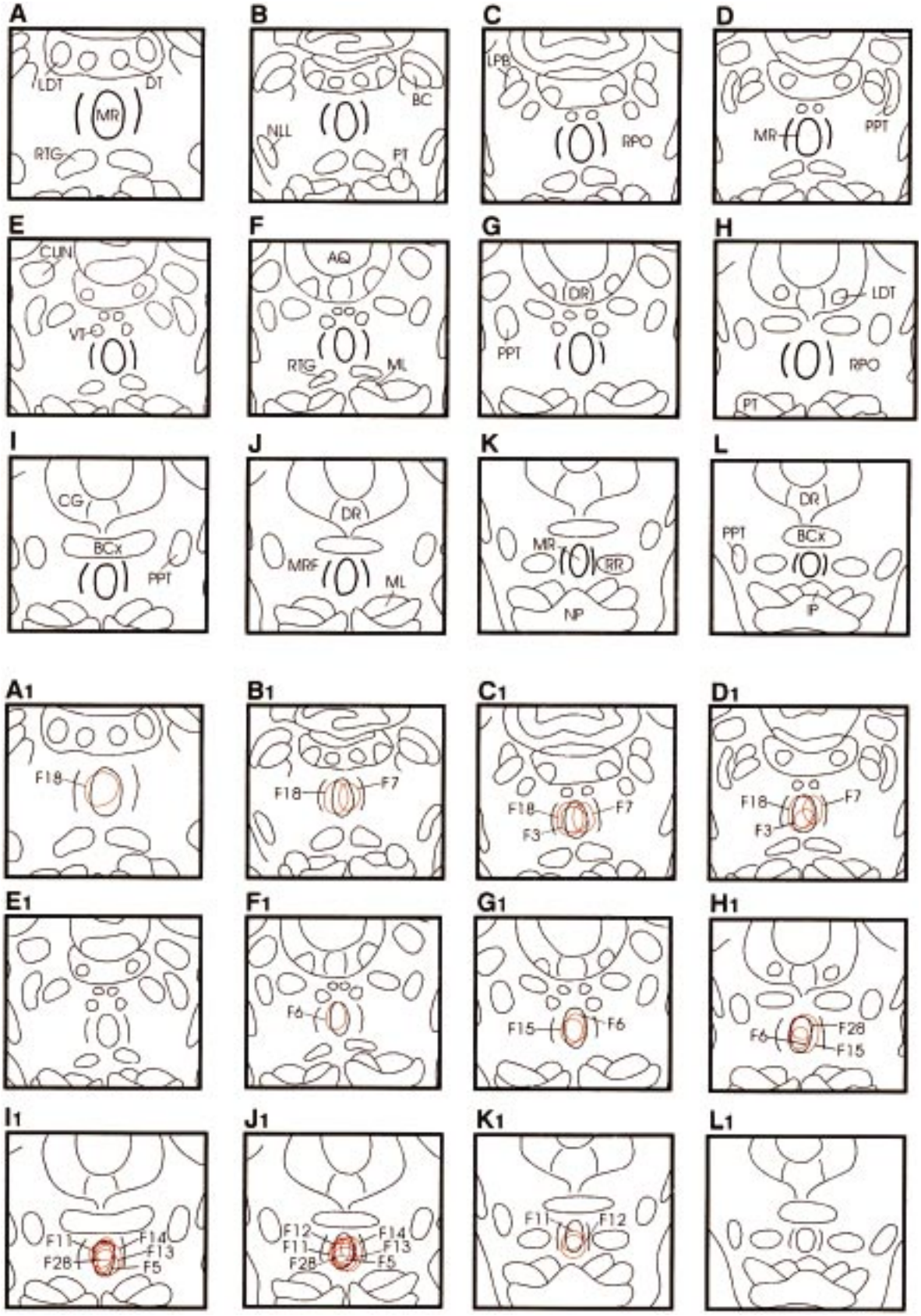

Fig. 2. **A–L:** A series of caudally to rostrally aligned (A to L) schematic transverse sections through the upper brainstem showing the location of the median raphe nucleus (bold). Sections are separated by 100 µm. **A_1–L_1:** A depiction in the same sections (A–L) of the locations of the first 11 injections (areas outlined in red) of 33 injections in the median raphe nucleus. The cases are F3, F5–F7, F11–F15, F18, and F28. Small injections are confined to one section; the largest injections span a maximum of four sections or approximately 400 µm. For abbreviations, see list.

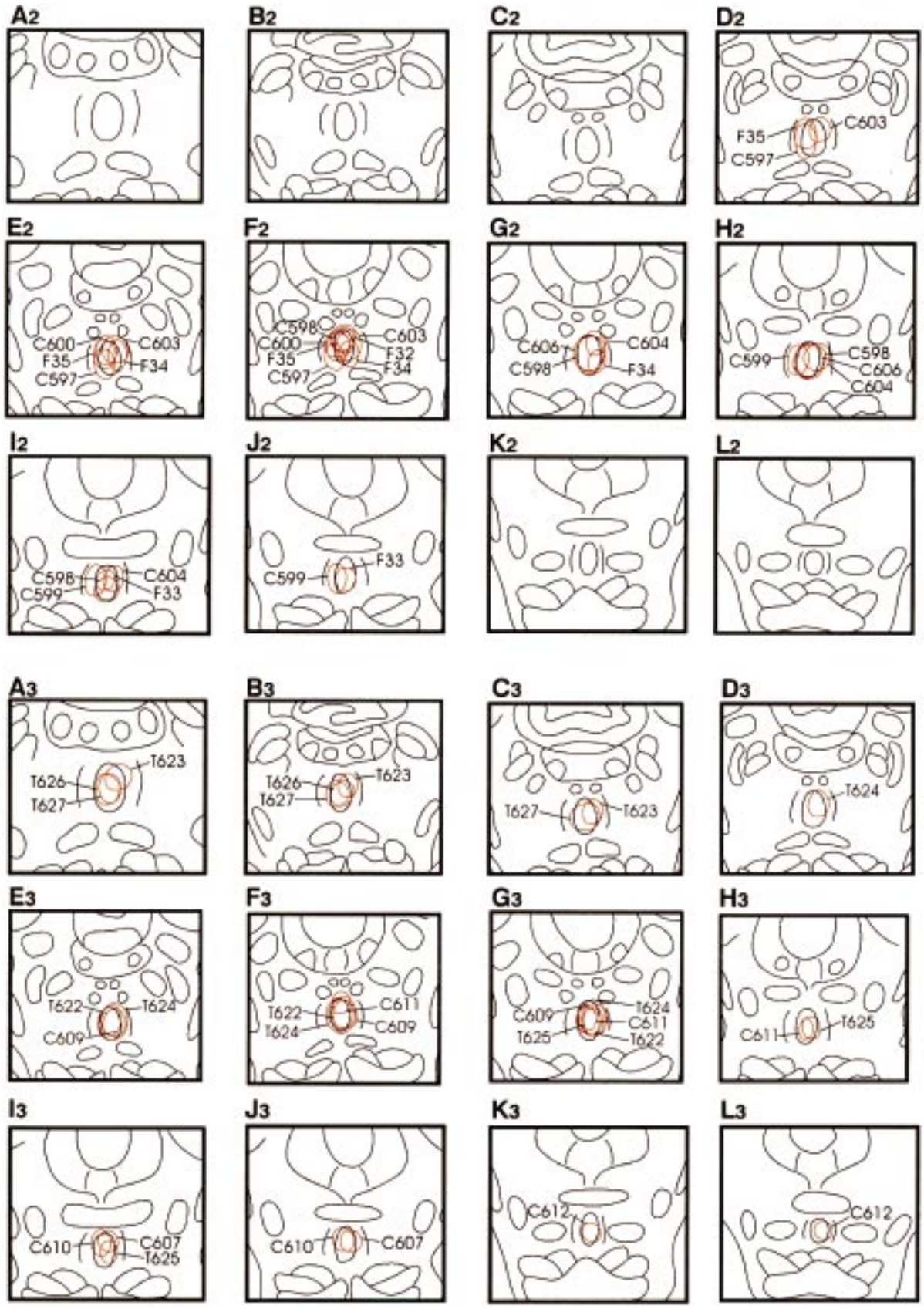

Fig. 3. Two series of schematic transverse sections through midbrain showing the locations (areas outlined in red) of the second (**A_2–L_2**) and third (**A_3–L_3**) series of 11 injections, respectively, of 33 injections in the median raphe nucleus. Sections are separated by 100 µm. The second series of cases are F32–F35, C597–C600, C603, C604; C606; the third series of cases are C607, C609–C612, T622–T627. Note that as a group (Figs. $2A_1$–L_1; $3A_2$–L_2; $3A_3$–L_3), the 33 injections span the caudorostral extent of MR. For abbreviations, see list.

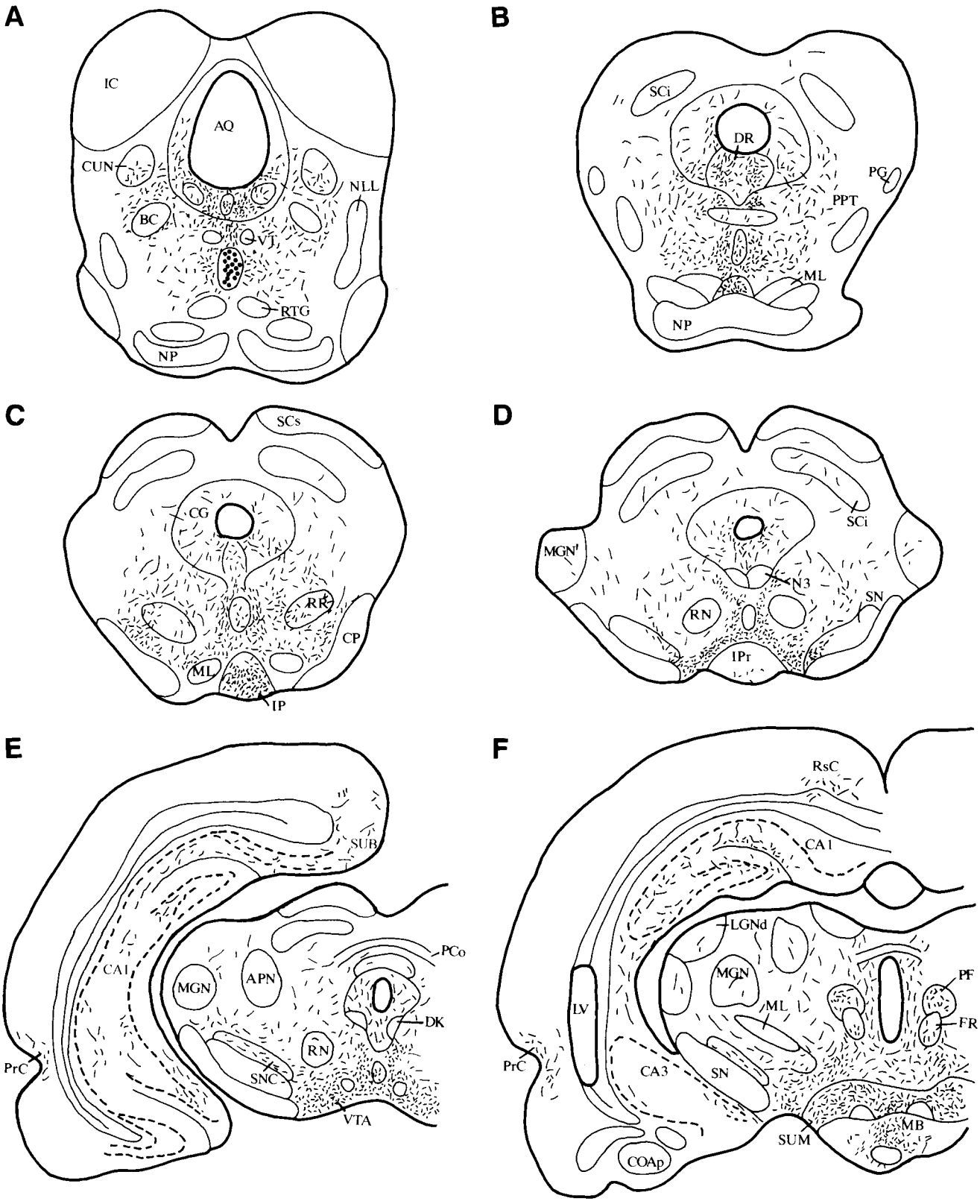

Fig. 4. **A–P:** Schematic representations of the labeling (dashed lines) present in selected sections through the rostral brainstem and forebrain produced by a PHA-L injection (dots in A) in the median raphe nucleus (case C606). For abbreviations, see list.

Figure 4 (Continued)

mainly passed through rather than terminated at the level of the rostral midbrain (Fig. 4D,E).

The principal target of labeled fibers at the caudal diencephalon (Fig. 4F) was the supramammillary nucleus (SUM). As depicted schematically (Fig. 4F) and in the photomicrographs of Figure 6, labeled fibers terminated densely throughout the extent of the SUM. Additional terminal sites included regions of the posterior hypothalamus overlying SUM, the medial mammillary body (MB), the periventricular gray (of thalamus), the parafascicular nucleus, zona incerta (ZI), VTA, and SNC. The dense collection of labeled fibers ventrolateral to FR represents the origin of the medial forebrain bundle (MFB) at the caudal hypothalamus. Labeled MR axons joined the MFB at this level and coursed with it through the diencephalon to the basal forebrain (Fig. 4F–L).

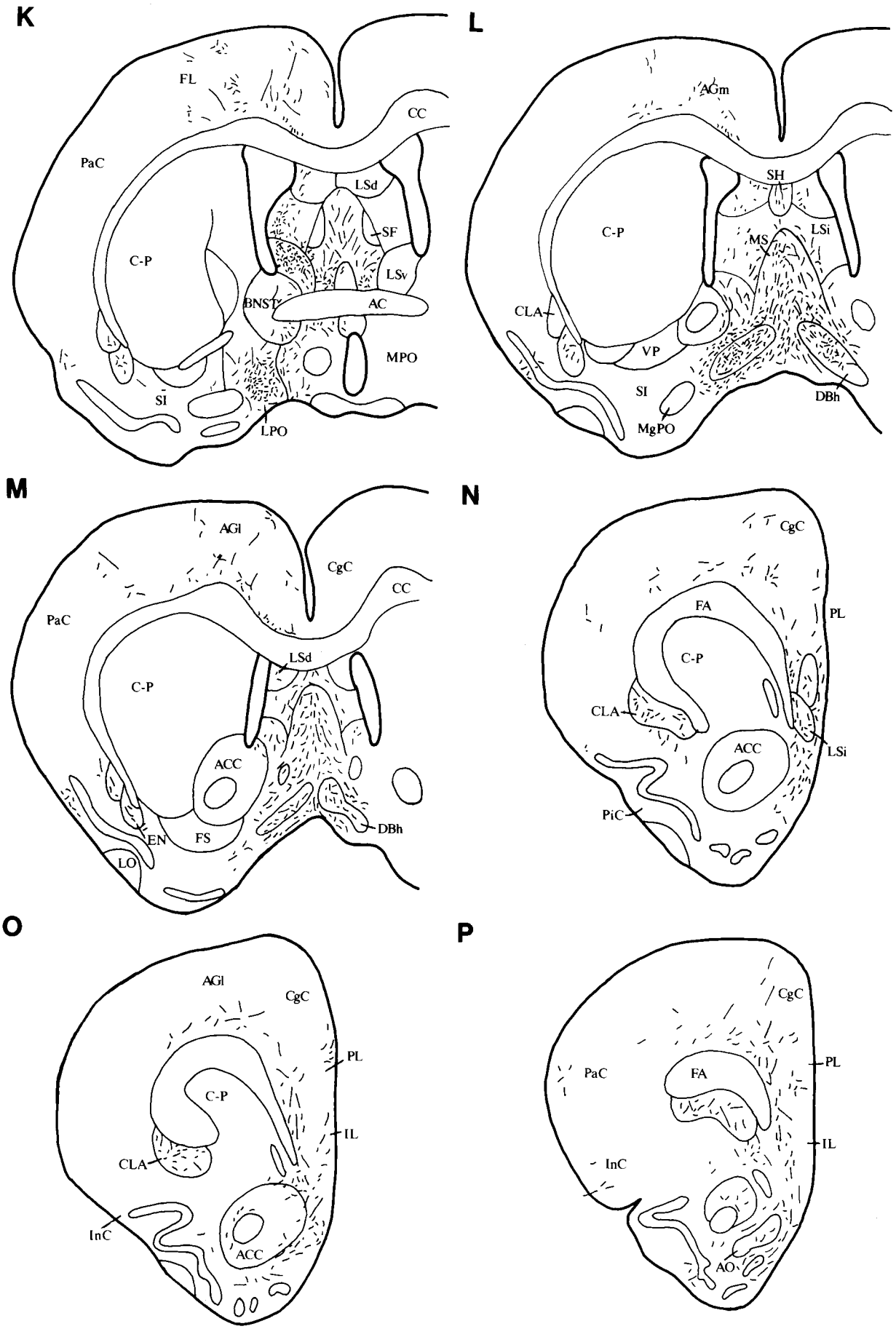

Figure 4 (Continued)

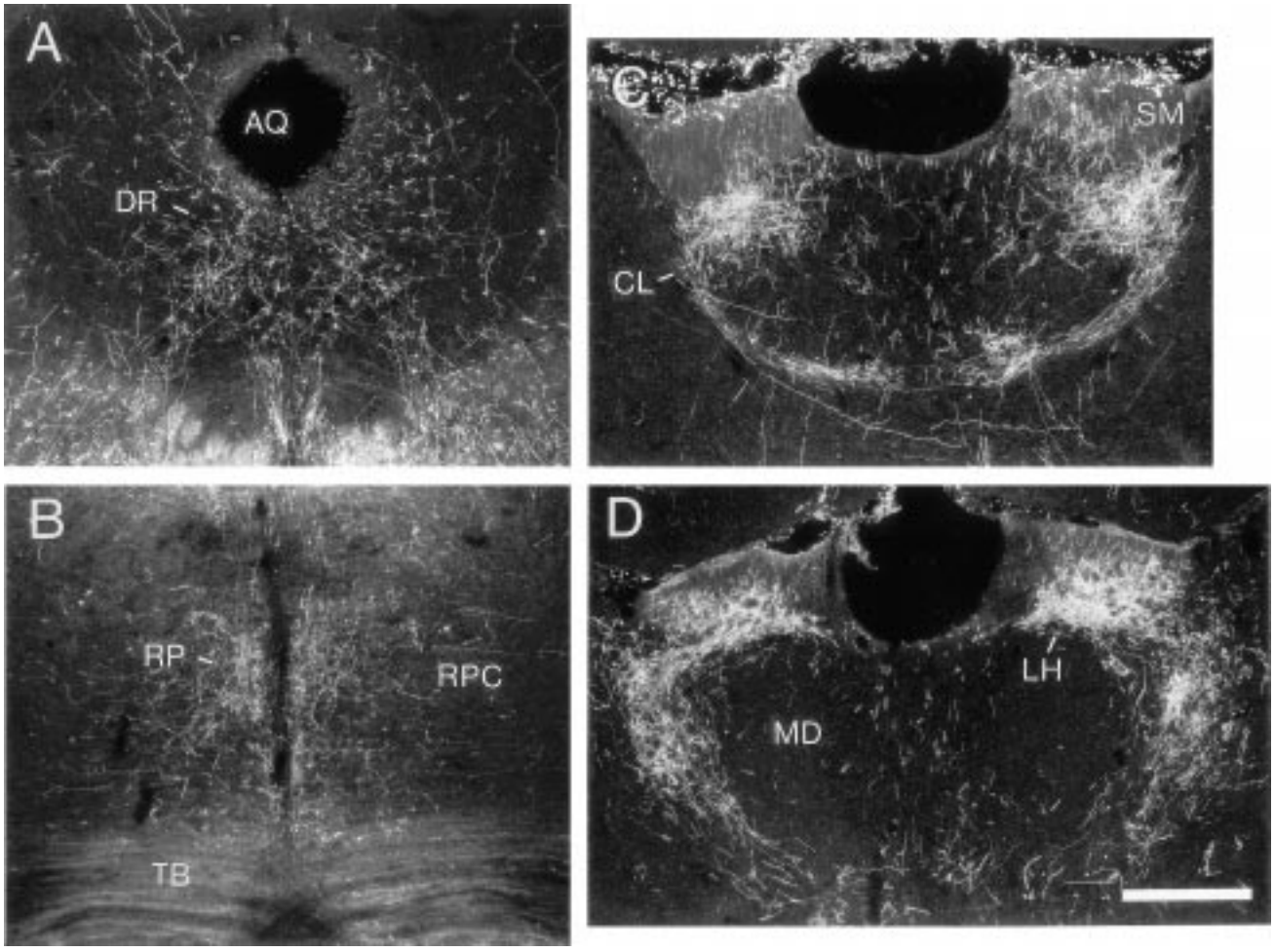

Fig. 5. Darkfield photomicrographs of transverse sections through the brainstem (A,B) and forebrain (C,D) showing patterns of labeling in the dorsal raphe nucleus and parts of the periaqueductal gray (**A**), the nucleus raphe pontis (**B**), the central lateral nucleus and medially adjacent mediodorsal nucleus of thalamus (**C**), and the lateral habenula (**D**) produced by the injection of case C606. For abbreviations, see list. Scale bar = 500 μm in D (applies to A–D).

Rostral to SUM, labeled fibers became largely segregated into dorsal and ventral clusters, with few fibers between the clusters (Fig. 4G,H). Labeled axons of the ventral cluster distributed (1) densely to the posterior nucleus of the hypothalamus (PH) (mainly its ventral half), the perifornical region (around the fornix) (Fig. 7) and an area directly below the mammillothalamic tract (Fig. 4G–I) that corresponds to the anteromedial ZI or to the dopamine-containing zone of ZI (Fig. 8); and (2) moderately to the periventricular, (i.e., bordering the third ventricle), lateral, and dorsomedial nuclei of the hypothalamus (Fig. 7). The principal targets of labeled axons of the dorsal cluster were the lateral habenula and the anterior intralaminar nuclei of the thalamus, mainly the central lateral nucleus (CL). The dense terminal labeling within LH and CL is depicted in the photomicrographs of Figure 5D and Figure 5C,D, respectively. The nucleus reuniens (RE), the laterodorsal and mediodorsal (lateral aspects) nuclei of thalamus, as well as the posterior and basomedial nuclei of the amygdala were lightly to moderately labeled. The ventromedial nucleus of the hypothalamus was devoid of labeled fibers (Figs. 4H,I and 7).

Similar to caudal levels of the diencephalon, only a few nuclei at the rostral diencephalon (Fig. 4I,J) were densely labeled; namely, the anteromedial ZI, [below the mammillothalamic tract (MT)] (Fig. 8), the intralaminar complex of thalamus (CL and to lesser degrees the paracentral and central medial nuclei) and the lateral habenula (LH). Apart from this, the dorsomedial nucleus of the thalamus (dorsomedial part), RE, and LHy were moderately labeled and only trace labeling was present within remaining sites at these levels.

The virtually sole destinations of labeled axons at the basal forebrain (Fig. 4K–M) were nuclei of the diagonal band (DB) and the medial and lateral septum. Caudally, labeled fibers exiting medially/dorsomedially from the MFB swept laterally around the anterior commissure into the septum to distribute terminally to the medial septal nucleus (MS) and to lateral parts of the lateral septum (LS). At the caudal levels of the septum (Fig. 4K), the LS was more densely labeled than the MS; the reverse was true at successively rostral levels of the septum (Fig. 4L,M). Within the LS, labeling was heaviest within the ventral nucleus (LSv) followed by the intermediate and

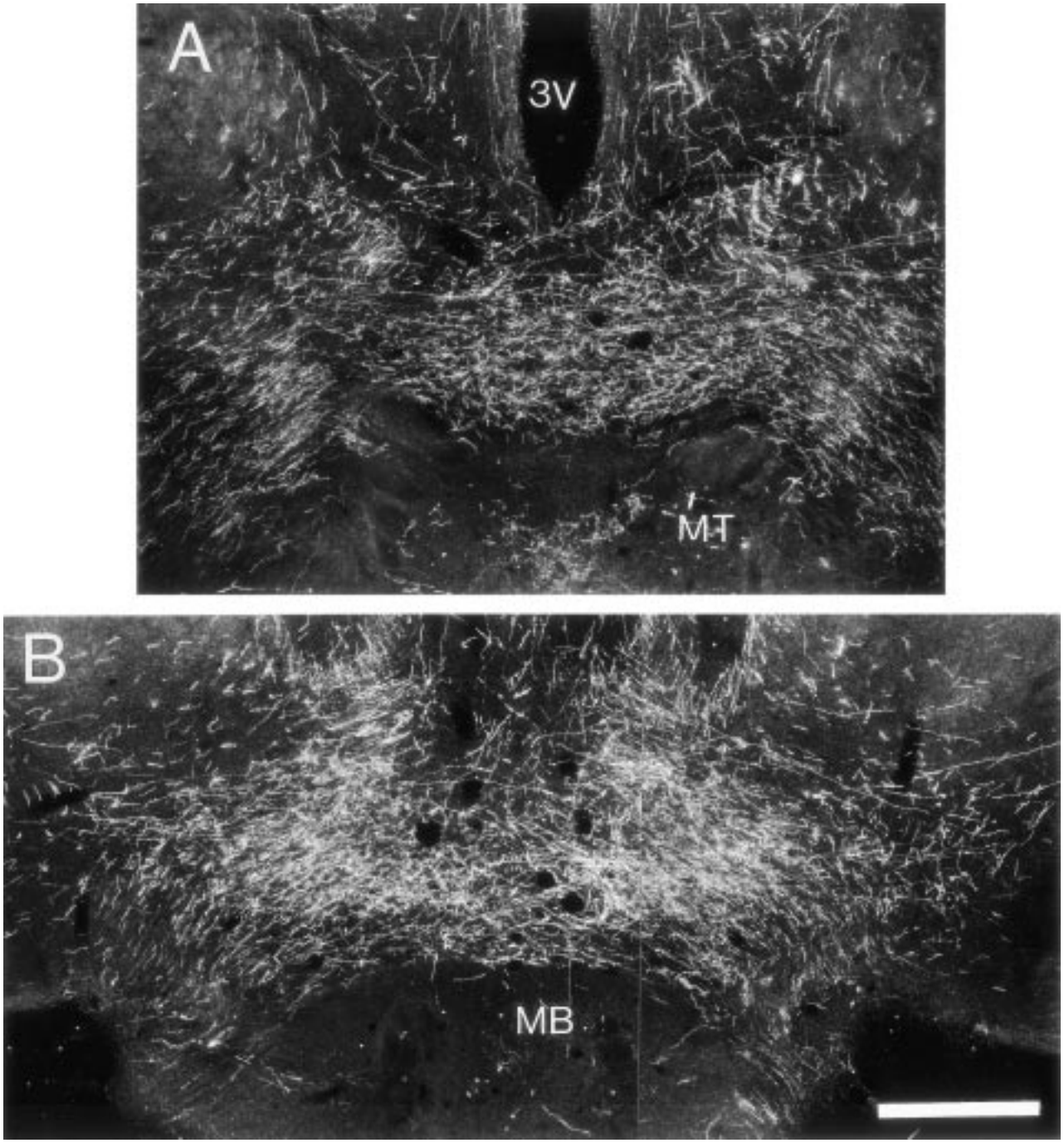

Fig. 6. Darkfield photomicrographs of transverse sections through the diencephalon showing patterns of labeling rostrally (**A**) and caudally (**B**) within the supramammillary nucleus (SUM) produced by the injection of case C606. Note strong labeling throughout SUM and most pronounced in the medial SUM and medial aspects of the lateral SUM. Scale bar = 500 μm in B (applies to A,B).

dorsal LS. At the rostral septum (Fig. 4L,M), labeled fibers were strongly bound for the DB (horizontal and vertical limbs) and MS, and to lesser degrees to the LS as well as dorsomedially to the septohippocampal nucleus. In addition to the septal complex, the endopiriform nucleus and the dorsally adjacent claustrum were lightly labeled (Fig. 4K–M). There was an essential absence of terminal labeling in several cell groups of the basal forebrain, including the preoptic nuclei (magnocellular, lateral and medial), the substantia innominata, the ventral pallidum and the bed nucleus of the stria terminalis.

Labeling thinned considerably at rostral levels of the forebrain (Fig. 4N–P) with most labeled fibers bound for regions of the frontal/prefrontal cortex. The rostral pole of

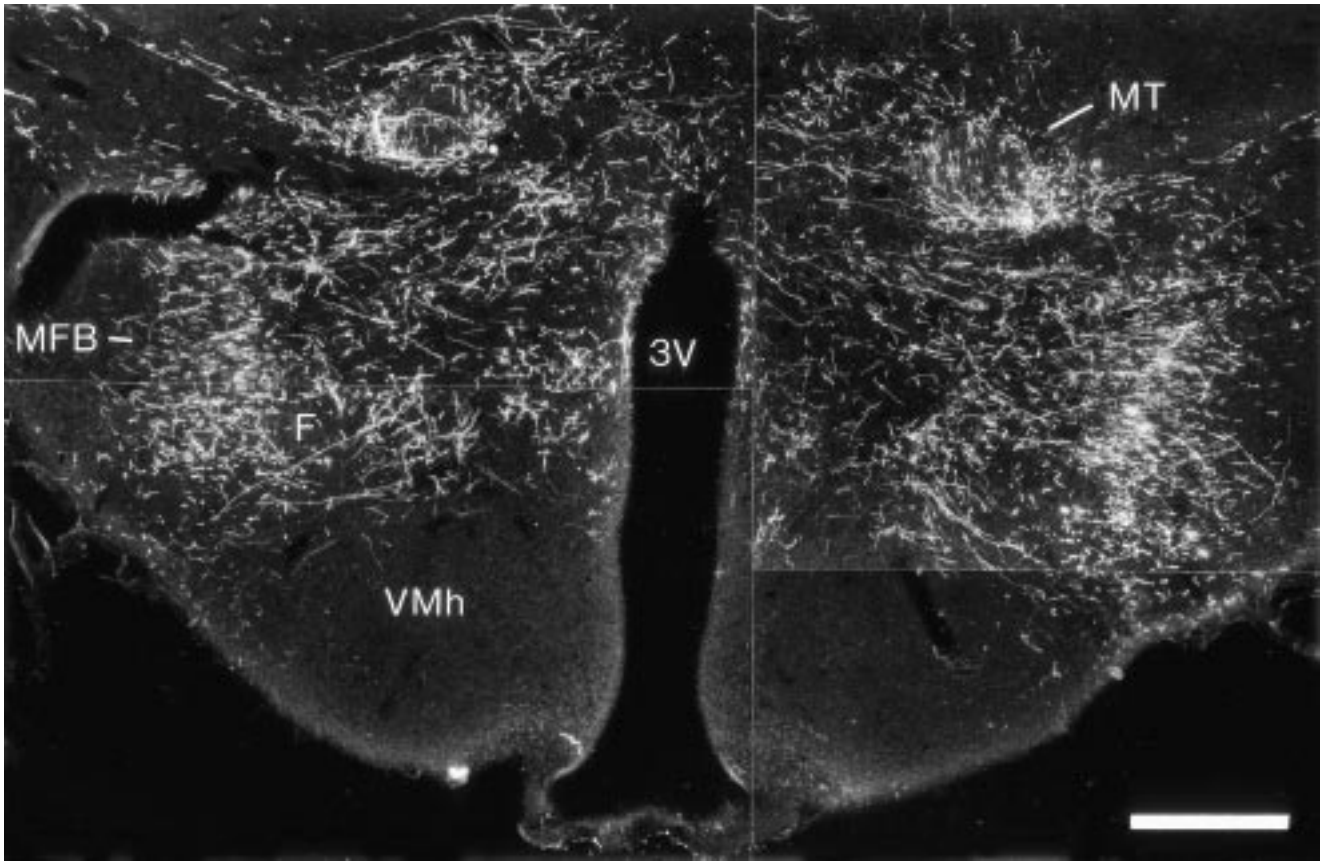

Fig. 7. Darkfield photomicrograph of a transverse section through the diencephalon showing labeled fibers in the medial forebrain bundle and distribution to several sites of the hypothalamus, including the dorsomedial hypothalamic area, the perifornical region, and the lateral hypothalamus. Note the absence of labeling in the ventromedial nucleus of the hypothalamus. Labeling produced by the injection of case C606. For abbreviations, see list. Scale bar = 500 μm.

LS and the rostral claustrum were lightly to moderately labeled; the nucleus accumbens was largely devoid of labeled axons.

Patterns of hippocampal and paleo/neocortical labeling

Hippocampal formation. Labeled fibers reached the hippocampus primarily through two routes: a main route through the fornix/fimbria, and a secondary route through the cingulum bundle. Labeled fibers of the main route ascended within the MFB to the basal forebrain, coursed dorsally/dorsomedially into the caudal septal area (Fig. 4K), joined the fornix (F) and fimbria (FI), and traveled caudally with F/FI to the hippocampus. Fibers of the secondary route also ascended within the MFB and rostrally within diagonal band to the anterior forebrain, coursed dorsomedially around the genu of the corpus callosum (CC), joined the cingulum bundle (CB), and traveled caudally with, and dorsal to, CB to the hippocampus (dorsal subiculum).

Overall, labeling was essentially moderate throughout the hippocampal formation (HF) for this case (C606) as well as for others with injections localized to the mid-to-caudal MR. This contrasts with dense labeling in the hippocampus observed with rostral MR injections (see case F14, below). Labeling was stronger in the dorsal (Fig. 4F–I) than in the ventral HF (Fig. 4E,F). The relatively small numbers of labeled fibers of the ventral HF mainly distributed to the dorsal part of subiculum, the outer molecular layers of CA1 and CA3 of Ammon's horn (dorsally and ventrally) and the stratum oriens of CA1 ventrally (Fig. 4E,F).

Within the dorsal HF, labeled axons terminated moderately throughout the rostrocaudal extent of outer molecular layers of CA1–CA3 as well as within the granule cell layer of the dentate gyrus (DG). Within Ammon's horn, labeling was densest within stratum lacunosum-moleculare of CA1, directly overlying the hippocampal fissure (Fig. 4F–I). Labeled axons of Ammon's horn were mainly oriented mediolaterally; a small percentage spanned the molecular layers, dorsoventrally. Within DG, labeling was tightly confined to the granule cell layer and immediately adjacent regions; labeling was stronger dorsally (suprapyramidal blade) than ventrally (infrapyramidal blade) in DG.

Paleo/neocortex. Overall, labeling was light throughout the cortex (paleo/neocortex) with this case (C606), as with all other MR cases. At caudal levels of the cortex, the only significantly labeled site was the perirhinal cortex (PrC). Labeled fibers distributed moderately throughout the extent of PrC; labeling was heaviest in the superficial layers (layers 1–3) of PrC. A few labeled fibers extended

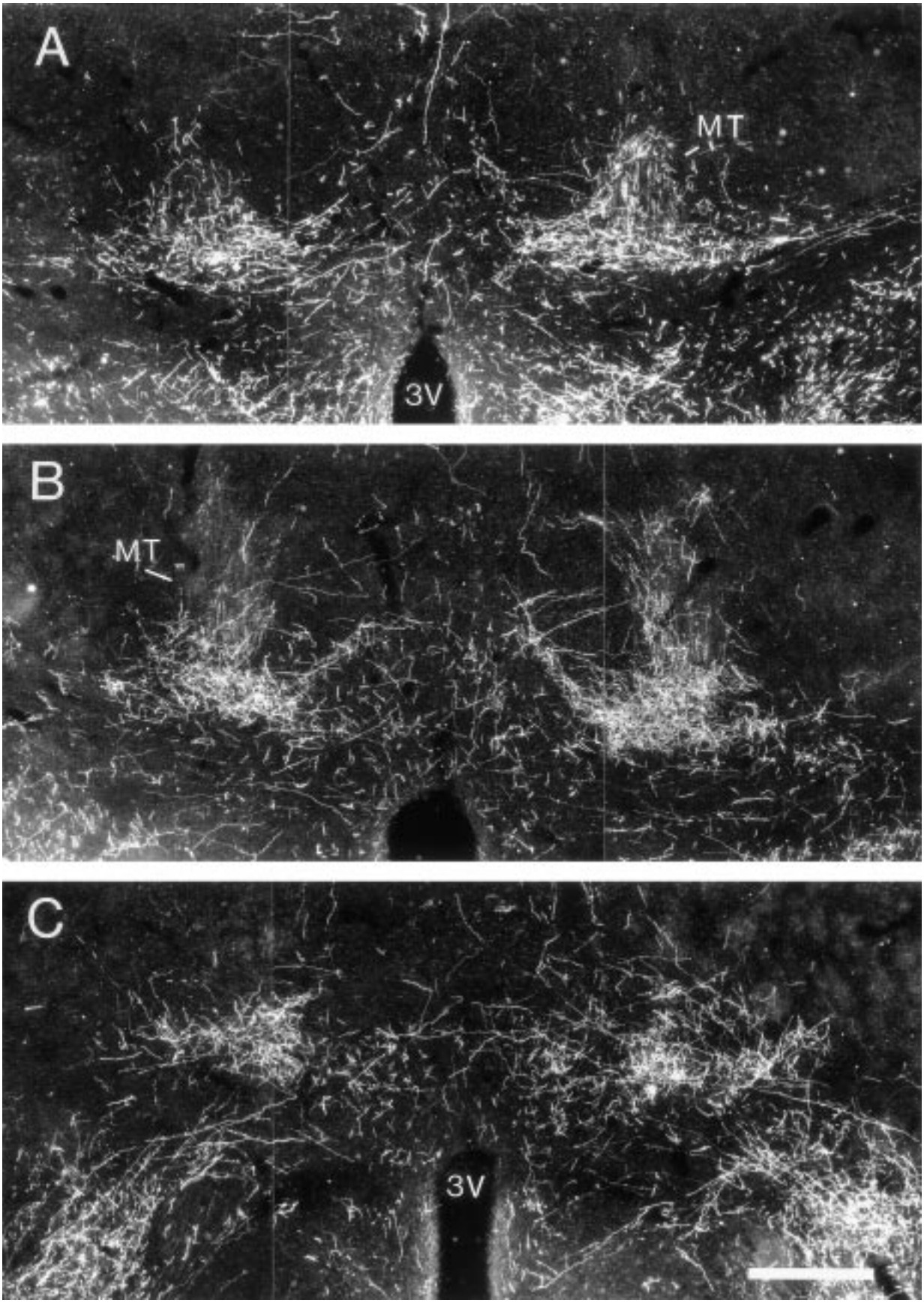

Fig. 8. Darkfield photomicrographs of transverse sections through the diencephalon showing dense terminal labeling with the medial zona incerta (ZI), directly below the mammillothalamic tract, at three caudal to rostral (**A–C**) levels of ZI. Labeling produced by the injection of case C606. Scale bar = 500 µm in C (applies to A–C).

dorsally and ventrally from PrC into the temporal and entorhinal cortices, respectively (Fig. 4G,H), and the limited numbers present in retrosplenial areas appeared mainly bound for the HF (see Fig. 4E).

The virtually exclusive targets of labeled fibers at the rostral levels of the cortex (Fig. 4J–P) were medial regions of the frontal/prefrontal cortex; namely, the medial and lateral agranular areas (AG_m and AG_l) as well as the anterior cingulate, prelimbic, and infralimbic cortices. This labeling appeared to be mainly terminal but involved some passage of labeled axons through this zone to caudal levels of the cortex and to HF. Labeling was stronger in deep than in superficial layers of each of these cortical regions.

Case C606: Descending projections

Figure 9 schematically depicts the distribution of labeled fibers in the pons and rostral medulla produced by a PHA-L injection in a mid-rostrocaudal part of MR (case C606). Labeled fibers from the site of injection (Fig. 4A) primarily descended along the midline to mainly distribute at the mid-pons to the pontine CG and along the course of their descent to nucleus raphe pontis (RP) (Fig. 9A). Within the CG, the dorsolateral tegmental nucleus was densely labeled, the nucleus incertus (INC) moderately labeled, and the locus coeruleus (LC) lightly labeled. Labeled fibers encircled but none terminated within the dorsal tegmental nucleus (of Gudden). Outside of CG, labeled axons distributed densely to RP (Figs. 5B, 9A), moderately to the medial parabrachial nucleus and at best lightly throughout remaining regions of the tegmentum including the pontine RF (nucleus pontis caudalis). Only trace labeling (i.e., a few positively stained axons in the motor nucleus of the trigeminal nerve) (see Fig. 9B) was observed in the sensory/motor cranial nerve nuclei at this or more caudal levels of the brainstem.

The main targets of labeled fibers at the caudal pons/rostral medulla (Fig. 9B), similar to the mid-pons (Fig. 9A), were parts of the CG and the midline raphe group nucleus raphe magnus (RM). Aside from the rather dense collections of labeled axons along the midline beginning dorsally in INC and continuing ventrally to RM, only scattered labeling was seen throughout the rest of the tegmentum. The LC and nucleus pontis caudalis (RPC) were sparsely to lightly labeled.

Labeling thinned considerably further caudally within the brainstem (rostral-to-mid medulla) (Fig. 9C,D). The relatively few labeled fibers still present at these levels terminated lightly to moderately within RM as well as midline regions dorsal to it, and sparsely within the nucleus gigantocellularis (NGC) and nucleus gigantocellularis, pars α (NGCa). Only sporadic labeling was observed with this case (and all other MR cases) within the lower brainstem (mid-to-caudal medulla).

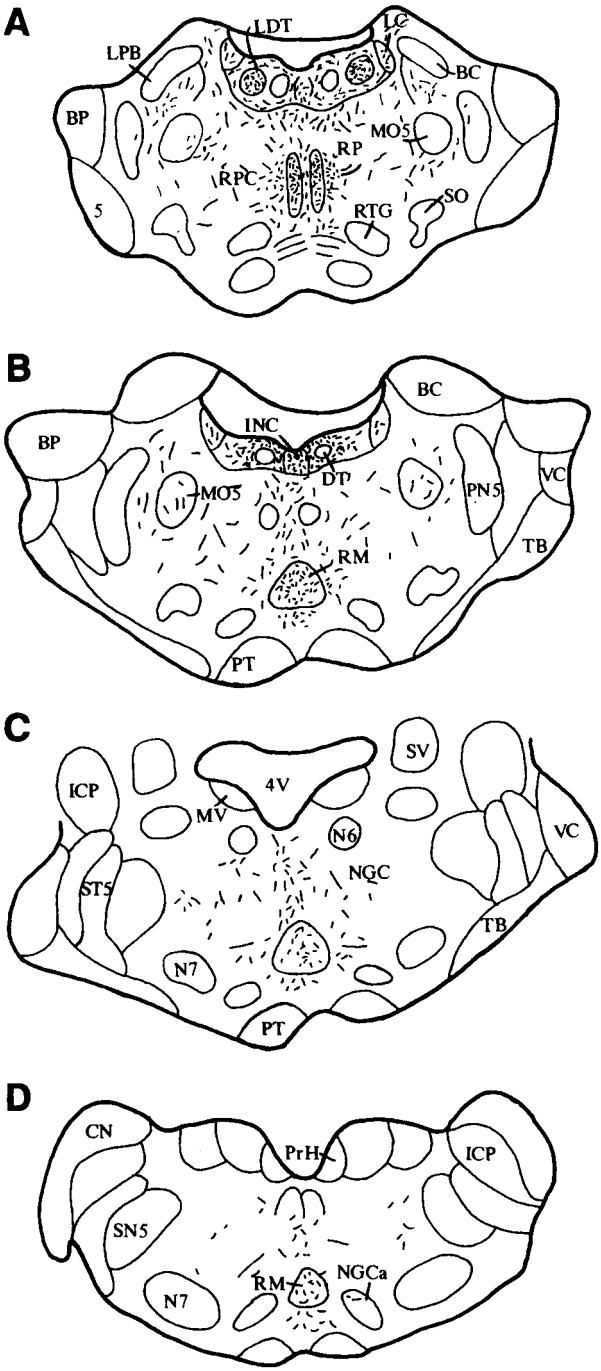

Fig. 9. **A–D:** Schematic representations of the labeling present in selected sections through the brainstem produced by a PHA-L injection of case C606. For abbreviations, see list.

Case F14: Patterns of labeling in the septum and hippocampal formation

Septum. Figure 10 schematically depicts the pattern of distribution of labeled fibers throughout the medial and lateral septum produced by a PHA-L injection in the rostral part of MR (case F14). Caudally (Fig. 10A), labeled fibers exited dorsally from the MFB, curved laterally around the anterior commissure (AC), skirted the lateral edge of the fornix, and either continued rostrally through the septum or terminated at the caudal septum, mainly within LS. The ventral nucleus of LS contained a dense aggregation of labeled fibers; progressively fewer were observed in the LSi and LSd.

Further rostrally (Fig. 10B,C), labeled axons continued to pass from the MFB into the septum, distributing densely (1) throughout the extent of MS; and (2) to lateral aspects of the LS (LSd, LSi, and LSv), following the contour of the septum. There was an essential absence of

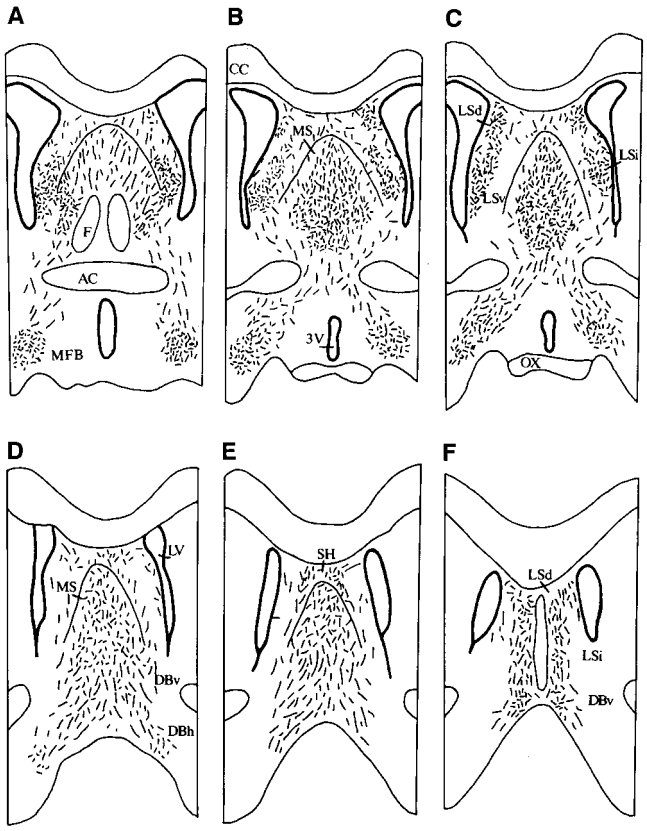

Fig. 10. **A–F:** Schematic representations of the labeling present in selected sections through the septum produced by a PHA-L injection in the rostral MR (case F14). For abbreviations, see list.

labeling in the medial LS. This pattern of labeling is depicted in the photomontage of Figure 11.

At rostral levels of the septum (Fig. 10D,E), labeling remained pronounced medially but diminished laterally. The medial septum, the dorsally adjacent septohippocampal nucleus as well as the ventrally adjacent ventral limb of the diagonal band nucleus (DBv) were densely labeled; the LS (LSd, LSi, and LSv) was lightly labeled. The labeled axons at the rostral pole of the septum (Fig. 10F) appeared mainly bound for the anterior basal forebrain and cortex; some distributed terminally to the septohippocampal nucleus (SH), MS, DBv, and medial aspects of LS.

Hippocampal formation. Figures 12 and 13 schematically depict the pattern of distribution of labeled fibers throughout the hippocampal formation (and parts of the cortex) produced by a PHA-L injection in the rostral part of MR (case F14). Labeling at caudal levels of the HF (Fig. 12A–C) was primarily restricted to the entorhinal cortex (EC); labeled axons spread throughout all layers of EC, distributing moderately to the lateral EC and less so to the medial EC. A few labeled fibers were present in the parasubiculum, presubiculum, and temporal parts of the subiculum.

Further rostrally within the ventral hippocampus (Fig. 12D), labeled fibers reaching the hippocampus dorsally from the retrosplenial cortex and ventrally from EC distributed lightly to moderately to dorsal and ventral regions of the subiculum, and sparsely to CA1. The dense collections of labeled fibers in DG were concentrated within the granule cell layer of the upper and lower blades of DG, the entire hilar region and the molecular layer immediately adjacent to the upper blade of DG.

Labeling became progressively stronger at successive rostral levels of the ventral HF. Labeled axons virtually blanketed Ammon's horn and DG at rostral levels of the ventral HF (Fig. 12E,F). A dense, continuous column of labeled axons following the curvature of the hippocampus was found to line the outer molecular layers of Ammon's horn, adjacent to the fissure, beginning dorsally in CA1 and continuing to the ventral subiculum. Labeling was densest in stratum lacunosum-moleculare. A parallel band extended dorsoventrally throughout the molecular layer of CA3, abutting the polymorphic layer of the upper blade of DG. The stratum pyramidale and stratum oriens (CA1–CA3) were lightly to moderately labeled.

Within DG, labeled fibers terminated heavily in the inner polymorphic layer of the upper blade of DG, and significantly but less so in the granule/polymorphic layer of the lower blade of DG (Fig. 12E,F). The molecular layers of the upper and lower blades of DG were moderately labeled. The foregoing pattern of labeling is depicted in the photomontage of Figure 14.

Similar to the rostro-ventral hippocampus, labeling was dense throughout the dorsal hippocampus (Figs. 13A–D, 15). Mirroring their distribution in the ventral HF, labeled fibers of Ammon's horn of the dorsal HF terminated densely within a relatively narrow zone (approximately 100 μm in diameter) in the outer molecular layers of CA1–CA3 and moderately within strata pyramidale and oriens of CA1–CA3. Labeling was heavier laterally than medially in Ammon's horn of the dorsal HF.

Comparable to Ammon's horn, labeled fibers distributed heavily throughout the rostrocaudal extent of DG of the dorsal HF. A tight band of labeled fibers terminated strongly in the granule cell layer and immediately adjacent molecular/polymorphic layers of the upper blade of DG and heavily, but less intensely, in these regions of the lower blade of DG. The outer molecular zones of the upper and lower blades of DG were lightly labeled.

DISCUSSION

This report represents a comprehensive examination of the projections of the median raphe nucleus by using the anterograde anatomical tracer, PHA-L. In the following, we highlight our results, compare them with those of previous studies, and discuss functional implications.

The main ascending bundle of labeled fibers from MR courses rostrally from the MR just lateral to the midline, turns ventrally, and spreads mediolaterally across the ventral tegmentum at the rostral midbrain, joins the medial forebrain bundle (MFB) at the caudal diencephalon, and continues with it to the basal forebrain. MR fibers primarily course within medial aspects of the MFB. The MFB (Azmitia and Segal, 1978; Vertes, 1984) and specifically the medial MFB (Nieuwenhuys et al., 1982; Veening et al., 1982; Geeraedts et al., 1990a,b) has previously been identified as the main ascending route for MR fibers.

The patterns of subcortical and cortical labeling produced by PHA-L injections into the MR are summarized in Table 1 and Figure 16A. As described, MR fibers predominantly distribute to midline/para-midline structures; that is, caudally to the midline raphe nuclei and to medial regions of the CG, and rostrally to such midline structures

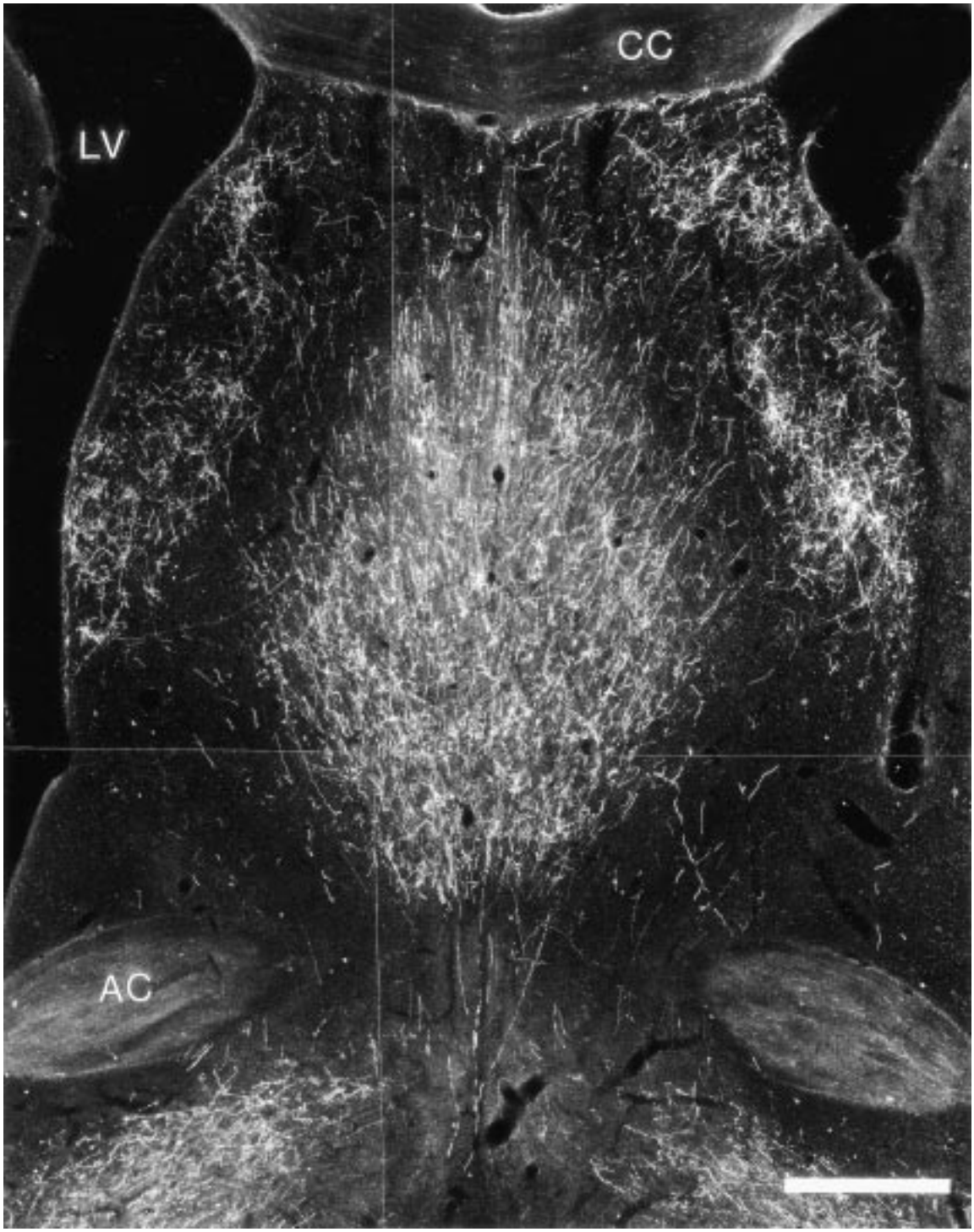

Fig. 11. Darkfield photomicrograph through the rostral forebrain showing pattern of labeling in the medial and lateral septum produced by the injection of case F14. Note pronounced labeling in the medial septum and lateral part of the lateral septum (LS) but an essential absence of labeling in the medial part of the LS. For abbreviations, see list. Scale bar = 500 μm.

as the interpeduncular nucleus, the medial mammillary body, the supramammillary nucleus, the posterior nucleus of the hypothalamus, the midline and intralaminar nuclei of thalamus, the medial zona incerta, the lateral habenula, the diagonal band nuclei, the medial septum, and hippocampus. This pattern of distribution significantly differs from that of the dorsal raphe nucleus (Vertes, 1991). As will be discussed, the MR and DR distribute to essentially nonoverlapping regions of the forebrain, indicating that the 5-HT innervation of the forebrain is shared by the MR

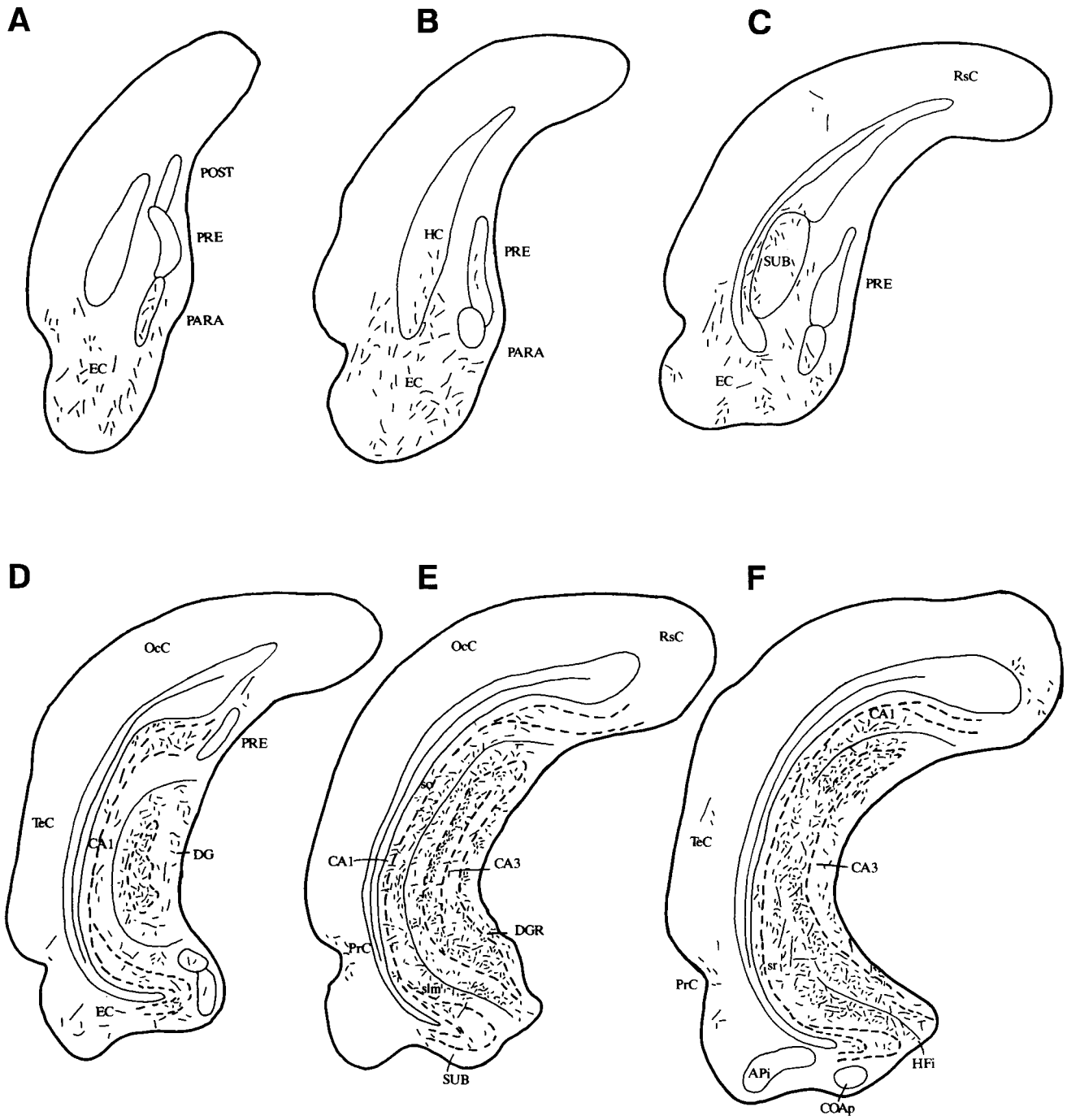

Fig. 12. **A–F:** Schematic representations of the labeling present in selected sections through the ventral hippocampal formation and entorhinal cortex produced by a PHA-L injection in the rostral MR (case F14). For abbreviations, see list.

and DR. Structures of the forebrain receive projections predominantly from the MR or DR but not from both nuclei.

Comparisons of projections from caudal and rostral parts of MR

There were no major differences in patterns of projections from caudal and rostral parts of MR, essentially only differences in relative densities of projections to some sites: stronger caudal than rostral MR projections to the brainstem, hypothalamus (particularly the mammillary body, SUM, and PH), and zona incerta; and stronger rostral than caudal MR projections to the diagonal band nuclei, septum, and hippocampus (compare Fig. 4 with Figs. 10, 12, 13). The interpeduncular nucleus, LH and the thalamus received essentially equivalent projections from caudal and rostral parts of the MR.

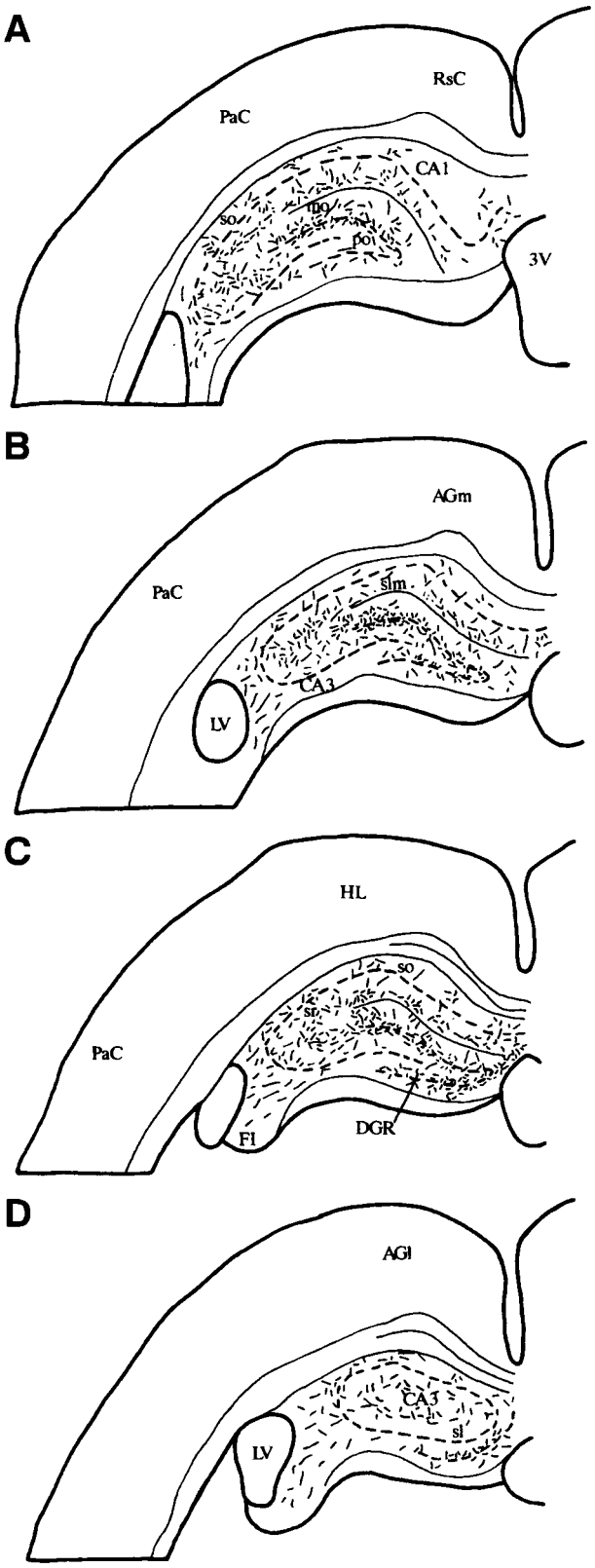

Fig. 13. **A–D:** Schematic representations of the labeling present in selected sections through the dorsal hippocampal formation produced by a PHA-L injection in the rostral MR (case F14). For abbreviations, see list.

Major MR projection sites in brainstem: Comparisons with previous studies

Laterodorsal/pedunculopontine tegmental nuclei. MR distributes densely to laterodorsal tegmental nuclei (LDT) and moderately to pedunculopontine tegmental nuclei (PPT) (Figs. 4, 9; Table 1). Interest in LDT/PPT stems from the presence of cholinergic neurons in the LDT/PPT and the involvement of LDT/PPT in the control of events of rapid eye movement (REM) (pontogeniculo-occipital spikes and cortical EEG desynchronization) and the state of REM sleep (for review, Leonard and Llinas, 1990; Vertes, 1990; Jones, 1991, Datta, 1995). In accord with the present findings, injections of retrograde tracers in LDT or PPT have been shown to produce pronounced retrograde cell labeling in MR (Cornwall et al., 1990; Semba and Fibiger, 1992; Steininger et al., 1992).

A recent examination (Steininger et al., 1997) of dorsal raphe projections to LDT/PPT provided indirect evidence for serotonergic MR projections to LDT/PPT. Steininger et al. (1997) described greater numbers of 5-HT fibers innervating LDT/PPT than those originating from the DR, indicating an alternative source of 5-HT projections to these sites, putatively from MR.

Although the DR is thought to be the primary (or sole) source of serotonergic influences on LDT/PPT in the control of sleep/sleep state functions, the present demonstration of relatively significant MR projections to LDT/PPT, together with the findings that 5-HT MR neurons, like those of the DR, fire at progressively lower rates from waking to SWS to REM (Rasmussen et al., 1984; Jacobs and Azmitia, 1992) suggests that the MR may participate with the DR in the control of these functions.

Reticular formation. MR fibers distribute lightly to moderately throughout the core of the medial brainstem reticular formation (RF) and sparsely to the lateral parvocellular RF (Fig. 9; Table 1). Early autoradiographic studies confirm present findings of moderately dense MR projections to the medial RF (Conrad et al., 1974; Bobillier et al., 1976, 1979; Vertes and Martin, 1988). By contrast, a number of reports that used retrograde techniques have described minimal MR projections to the RF (Gallager and Pert, 1978; Shammah-Lagnado et al., 1983, 1987; Bayev et al., 1988; Kobayashi et al., 1994). For instance, Shammah-Lagnado and colleagues (Shammah-Lagnado et al., 1983, 1987) identified few retrogradely labeled cells in MR after HRP/WGA-HRP injections in RPC, RPO, or the MRF, and Kobayashi et al. (1994), examining 5-HT afferents to the medial pontomedullary RF, concluded that most (5-HT fibers) arise from the pontine CG, and few, if any, from the MR.

At variance with the foregoing retrograde reports, Semba (1993) described pronounced 5-HT projections to the pontine RF, and showed that approximately one-third originate from the MR. The retrograde tracer injections of Semba (1993) appeared anterior and medial to those of other studies (Shammah-Lagnado et al., 1987; Kobayashi et al., 1994), and, as shown here, MR fibers distribute significantly to the anteromedial RF and progressively less so to caudal/lateral regions of RF.

Central gray. MR fibers distribute moderately throughout the longitudinal extent (pons through diencephalon) of central gray (CG), and most densely ventrally/ventromedially in CG in and/or around specific nuclei of the ventral CG: INC, LDT, DR (Figs. 4, 9; Table 1).

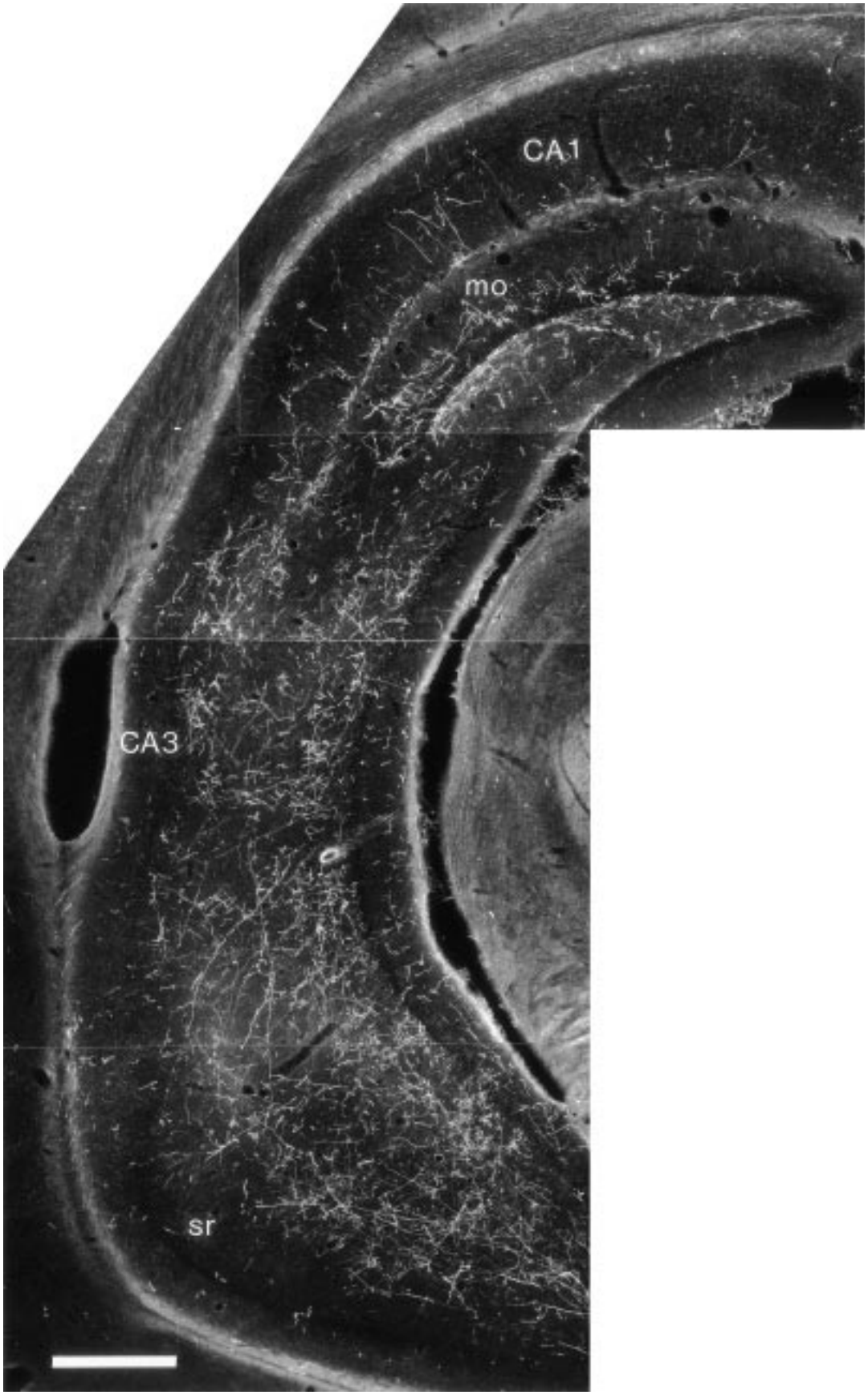

Fig. 14. Darkfield photomicrograph showing pattern of labeling in the ventral hippocampal formation produced by the injection of case F14. Note pronounced terminal labeling throughout molecular layers of CA3 and ventral CA1. For abbreviations, see list. Scale bar = 500 μm.

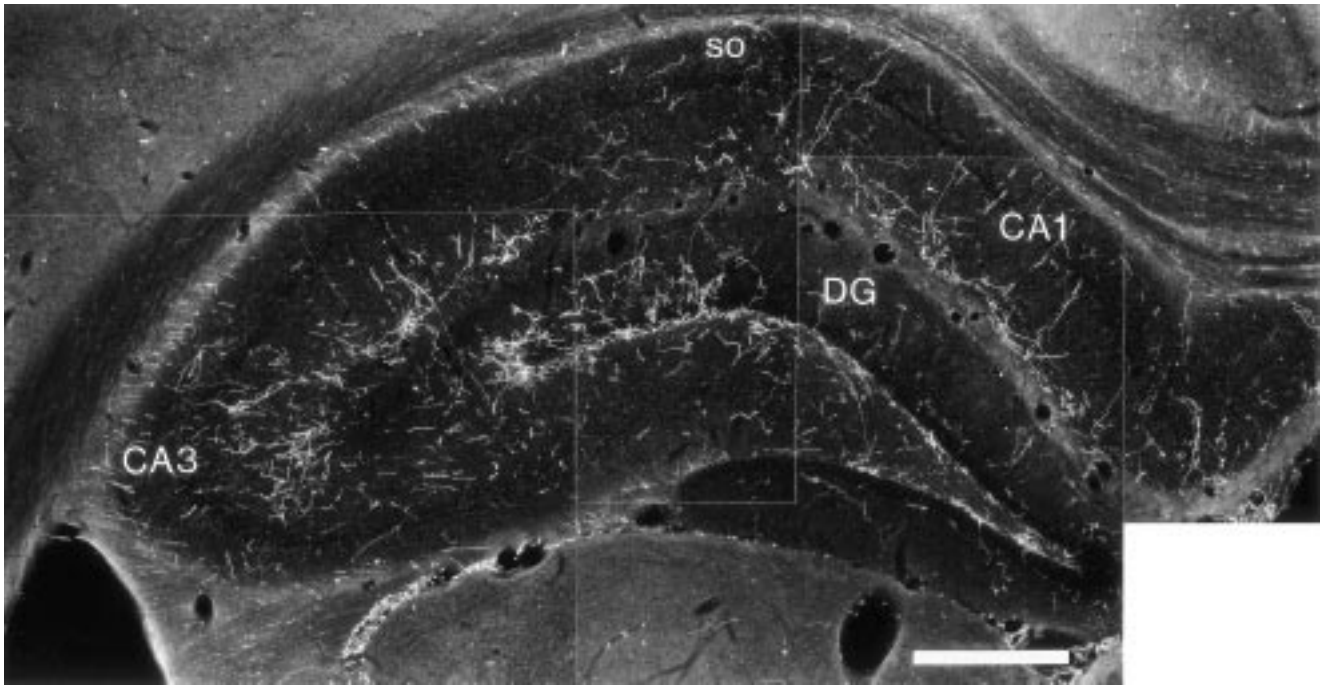

Fig. 15. Darkfield photomicrograph showing pattern of labeling in the dorsal hippocampal formation produced by the injection of case F14. Note dense terminal labeling in the outer molecular layers of CA1–CA3 as well as in the granule cell layer and adjacent molecular layers of the upper and lower blades of the dentate gyrus. For abbreviations, see list. Scale bar = 500 μm.

Previous reports, that used various tracers, have similarly described relatively pronounced MR projections to CG, and as shown here, stronger projections to the ventral than to the dorsal CG (Conrad et al., 1974; Bobillier et al., 1976, 1979; Beitz, 1982; Beitz et al., 1986; Meller and Dennis, 1986; Vertes and Martin, 1988). The CG, particularly the ventral CG, is richly supplied by 5-HT fibers (Steinbusch, 1981; Parent et al., 1981; Clements et al., 1985). Beitz et al. (1986) demonstrated that approximately 12% of 5-HT fibers innervating CG originate from the MR and that about 50% of MR cells projecting to CG are serotonergic.

Dorsal raphe nucleus. MR fibers distribute moderately to densely throughout the extent of DR and strongest to the lateral wings of rostral DR (Figs. 4, 5A). Early reports demonstrated moderate cell labeling in MR after retrograde tracer injections in DR (Sakai et al., 1977; Kalen et al., 1988) and moderately dense terminal labeling in DR with autoradiographic injections in MR (Bobillier et al., 1976; Vertes and Martin, 1988). The DR sends a strong return projection to MR (Marcinkiewicz et al., 1989; Behzadi et al., 1990; Vertes and Kocsis, 1994). The pronounced reciprocal connections between MR and DR suggest a possible coordination of their activity during certain conditions or states, possibly leading to a fairly global release of 5-HT throughout the brain during these conditions.

Interpeduncular nucleus. MR projects strongly to the caudal two-thirds and lightly to the rostral one-third of interpeduncular nucleus (IP) (Fig. 4; Table 1). Several previous studies (Bobillier et al., 1976, 1979; Azmitia and Segal, 1978; Marchand et al., 1980; Contestabile and Flumerfelt, 1981; Hamill and Jacobowitz, 1984; Groenewegen et al., 1986; Shibata et al., 1986; Vertes and Martin, 1988) have reported that the IP is a major forebrain target of MR, and that MR fibers are mainly bound for the caudal IP (Groenewegen et al., 1986; Shibata et al., 1986). 5-HT neurons are present in the caudal IP (primarily in the apical and lateral subnuclei) (Hamill et al., 1984; Groenewegen et al., 1986), suggesting serotonergic MR to serotonergic IP interactions in the modulation of IP activity.

Major MR projection sites in forebrain: Comparisons with previous studies

Medial mammillary body and supramammillary nucleus. MR distributes densely to the medial mammillary body (MB) and to SUM (Figs. 4, 6; Table 1). The present findings of pronounced MR projections to MB confirm our previous demonstration of massive terminal labeling in medial MB after [^{3}H]leucine injections in MR (Vertes and Martin, 1988), as well as descriptions of significant numbers of labeled cells in MR after retrograde tracer injections in medial MB (Hayakawa and Zyo, 1984; Shibata, 1987; Allen and Hopkins, 1989).

Previous studies have demonstrated relatively moderate MR projections to SUM (Vertes and Martin, 1988; Hayakawa et al., 1993). The considerably stronger MR-SUM projections demonstrated here than in these reports may involve the use of different tracers or size or locations of MR injections in the various studies.

Lateral habenula. MR fibers distribute massively throughout the extent of LH (Figs. 4, 5D; Table 1). This finding is consistent with previous reports showing that the LH is a major forebrain target of MR (Bobillier et al., 1976, 1979; Herkenham and Nauta, 1977; Azmitia and Segal, 1978; Vertes and Martin, 1988).

TABLE 1. Density of Labeling in Nuclei of the Brainstem and Forebrain Produced by PHA-L Injections in the Median Raphe Nucleus[1]

Structures	Labeling
Telencephalon	
Accumbens n.	+
Amygdala	
Anterior area	−
Basolateral	+
Basomedial	−
Central	+
Cortical	−
Medial	+
Lateral	−
Posterior	+
Bed n. of stria terminalis	+
Caudate-putamen	−
Claustrum	++
Cortex	
Cingulate	+
Entorhinal	++
Forelimb	+
Hindlimb	+
Infralimbic	+
Insular	−
Lateral agranular (motor)	+
Lateral orbital	−
Medial agranular (motor)	+
Occipital	−
Parietal	+
Perirhinal	++
Piriform	−
Prelimbic	+
Retrosplenial	+
Temporal	−
Diagonal band n.	
Horizontal limb	+++
Vertical limb	+++
Endopiriform n.	+
Globus pallidus	−
Hippocampal formation	
Ammon's horn	+++
Dentate gyrus	+++
Subiculum	++
Lateral septum	
Dorsal n.	+++
Intermediate n.	+++
Ventral n.	+++
Lateral preoptic area	++
Magnocellular preoptic n.	−
Medial preoptic area	+
Medial preoptic n.	−
Median preoptic n.	−
Medial septal n.	+++
Olfactory tubercle	−
Septohippocampal n.	+++
Substantia innominata	−
Ventral pallidum	−
Diencephalon	
Thalamus	
Anteromedial n.	+
Anterodorsal n.	+
Anteroventral n.	−
Central lateral n.	+++
Central medial n.	++
Intermediodorsal n.	+
Lateral geniculate n.	−
Lateral habenula	+++
Laterodorsal n.	+
Lateroposterior n.	−
Medial geniculate n.	−
Medial habenula	−
Mediodorsal n.	++
Paracentral n.	+++
Parafascicular n.	++
Paraventricular n.	+
Posterior n.	−
Reticular n.	−
Reuniens n.	++
Rhomboid n.	+
Submedial n.	−
Ventrolateral n.	−
Ventromedial n.	−
Ventral posterolateral n.	−
Ventral posteromedial n.	−
Hypothalamus	
Anterior n.	+
Dorsal hypothalamic area	+
Dorsomedial n.	+
Lateral n.	++

TABLE 1. (continued)

Structures	Labeling
Hypothalamus (continued)	
Mammillary bodies	+++
Paraventricular n.	−
Perifornical area	++
Posterior n.	+++
Premammillary n., dorsal	+
Premammillary n., ventral	−
Suprachiasmatic n.	+
Supramammillary n.	+++
Supraoptic n.	−
Ventromedial n.	−
Subthalamus	
Fields of Forel	++
Zona incerta	+++
Brainstem	
Abducens n.	−
Anterior pretectal n.	−
Barrington's n.	+++
Caudo-ventrolateral medulla	+
Central linear n.	++
Cuneate n.	−
Cuneiform n.	++
Dorsal cochlear n.	−
Dorsal motor n. vagus	−
Dorsal raphe n.	+++
Dorsal tegmental n.	−
Facial n.	−
Hypoglossal n.	−
Inferior colliculus	−
Inferior olive	−
Inferior vestibular n.	−
Interfascicular n.	++
Interpeduncular n.	+++
Kolliker-Fuse n.	+
Laterodorsal tegmental n.	+++
Lateral reticular n.	−
Lateral parabrachial n.	++
Lateral vestibular n.	−
Locus coeruleus	+
Medial parabrachial n.	+
Medial vestibular n.	−
Mesencephalic reticular formation	++
Motor trigeminal n.	−
N. ambiguus	−
N. incertus	+++
N. gigantocellularis	+
N. gigantocellularis, pars alpha	+
N. gigantocellularis, pars ventralis	−
N. lateral lemniscus	−
N. paragigantocellularis	−
N. pons	−
N. pontis caudalis	+
N. pontis oralis	++
N. posterior commissure	+
N. raphe magnus	+++
N. raphe obscurus	−
N. raphe pallidus	−
N. raphe pontis	+++
N. reticularis dorsalis	−
N. reticularis ventralis	−
N. solitary tract	−
N. trapezoid body	−
Parvocellular reticular n.	+
Pedunculopontine tegmental n.	++
Prepositus hypoglossal n.	−
Periaqueductal gray, midbrain	++
Periaqueductal gray, pons	++
Peripeduncular n.	+
Posterior pretectal n.	−
Principal trigeminal n.	−
Red n.	−
Reticular tegmental n. pons	−
Retrorubral area	++
Rostro-ventrolateral medulla	−
Spinal trigeminal n.	−
Substantia nigra, pars compacta	+
Substantia nigra, pars reticulata	−
Superior colliculus	+
Superior olive	−
Superior vestibular n.	−
Ventral cochlear n.	−
Ventral tegmental area	+++
Ventral tegmental n.	−

[1] +, light labeling; ++, moderate labeling; +++, dense labeling; −, absence of labeling; n, nucleus; PHA-L, *Phaseolus vulgaris*-leucoagglutinin.

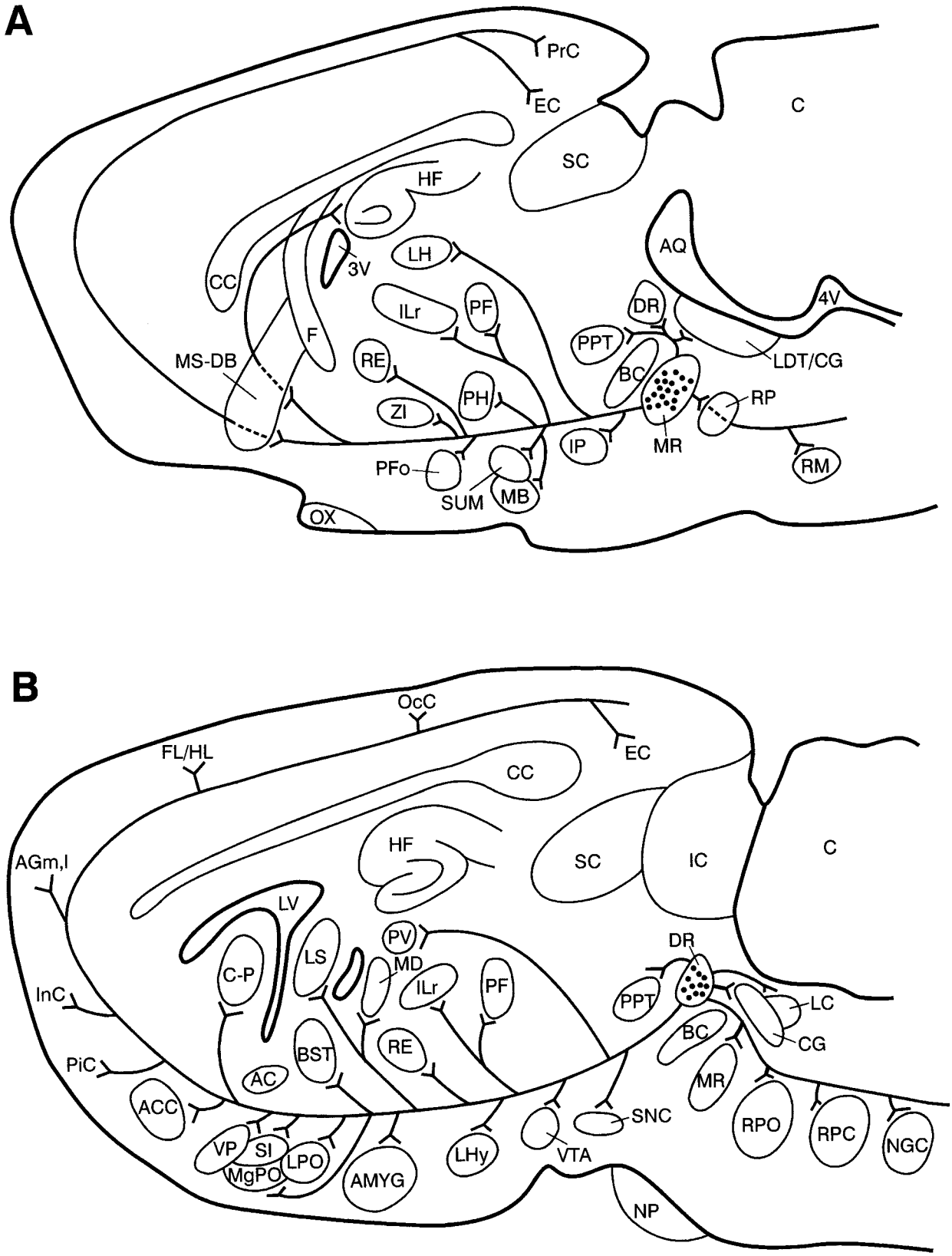

Fig. 16. **A:** A medial schematic sagittal section summarizing the principal projection sites of the median raphe nucleus. Dashed lines indicate fibers coursing through structures. **B:** For comparison with the principal projection sites of MR (A), a lateral schematic sagittal section summarizing the principal projection sites of the dorsal raphe nucleus (adapted from Vertes, 1991; Vertes and Kocsis, 1994). Dots in A and B represent labeled cells at sites of injection in the median and dorsal raphe nuclei, respectively. As illustrated, the MR and DR essentially project to nonoverlapping sites in the brainstem and forebrain (see text). Sections were modified from the rat atlas of Paxinos and Watson (1986). For illustrative purposes, a few sagittal sections are collapsed onto single sagittal planes in A and B. For abbreviations, see list.

The habenula has long been viewed as a important relay in descending systems linking the forebrain with the brainstem; i.e., a critical component of the limbic-midbrain circuit of Nauta (Nauta, 1958; Wang and Aghajanian, 1977, Herkenham and Nauta, 1979; Sutherland, 1982). Limbic (mainly septal) and striatal (mainly entopeduncular) afferents strongly converge on the habenula (Nauta, 1974; Herkenham and Nauta, 1977; Larsen and McBride, 1979; Sutherland, 1982), and efferents of the habenula are, in turn, mainly directed to the brainstem (Aghajanian and Wang, 1977; Herkenham and Nauta, 1979; Sutherland, 1982; Hamill and Jacobowitz, 1984; Groenewegen et al., 1986; Shibata et al., 1986; Araki et al., 1988). The medial habenula projects indirectly, by means of IP, to the brainstem; the lateral habenula directly to the brainstem (Aghajanian and Wang, 1977; Herkenham and Nauta, 1979; Maciewicz et al., 1981; Shibata and Suzuki, 1984; Sutherland, 1982; Groenewegen et al., 1986; Shibata et al., 1986; Araki et al., 1988; Marcinkiewicz et al., 1989; Behzadi et al., 1990).

The MR appears to be the primary target of LH fibers projecting to the brainstem (Aghajanian and Wang, 1977, Herkenham and Nauta, 1979; Maciewicz et al., 1981; Sutherland, 1982; Shibata and Suzuki, 1984; Groenewegen et al., 1986; Araki et al., 1988). These findings, together with present results showing massive MR to LH projections, indicate that the MR and LH are extensively interconnected and support the position that these structures are critical components of a limbic midbrain circuit of Nauta (1958) involved in the two-way transfer of information between the brainstem and forebrain.

Thalamus. MR fibers distribute unevenly to the thalamus; that is, densely to the central lateral nucleus; moderately to the thalamic CG, parafascicular (PF), paraventricular (PV), paracentral (PC), central medial (CM), reuniens and mediodorsal nuclei, and sparingly to remaining regions of thalamus (Figs. 4, 5C; Table 1). Consistent with this, early reports that used autoradiographic techniques described moderately dense MR projections to PF, PC, CL, CM, and PV, but few projections to other nuclei of thalamus (Bobillier et al., 1976, 1979; Azmitia and Segal, 1978; Vertes and Martin, 1988).

Retrograde examinations of afferents to thalamus have yielded similar results. Significant numbers of labeled cells have been identified in MR after retrograde tracer injections in PV (Cornwall and Phillipson, 1988b; Chen and Su, 1990), the mediodorsal nucleus (MD) (Velayos and Reinoso-Suarez, 1982; Cornwall and Phillipson, 1988a; Groenewegen, 1988; Newman and Ginsberg, 1994) and the rostral intralaminar complex (Carstens et al., 1990; Newman and Ginsberg, 1994); but few, if any, with injections in PF-CM (McGuinness and Krauthamer, 1980; Comans and Snow, 1981; Nakano et al., 1985; Royce et al., 1991), RE (Herkenham, 1978); ventromedial (VM) (Herkenham, 1979; Jimenez-Castellanos and Reinoso-Suarez, 1985; Nakano et al., 1985, Newman and Ginsburg, 1994), ventrolateral (VL) (Nakano et al., 1985, Newman and Ginsburg, 1994), or the ventrobasal complex (Carstens et al., 1990; Newman and Ginsberg, 1994).

The nucleus submedius (SME), a thalamic nucleus associated with nociception, (Craig and Burton, 1981) is richly innervated by 5-HT fibers (Matsuzaki et al., 1993). Although MR was initially thought to be a prominent source of 5-HT afferents to SME (Peschanski and Besson, 1984; Coffield et al., 1992; Yoshida et al., 1992), recent findings of Matsuzaki et al. (1993), and present results, indicate that the raphe input to SME virtually entirely originates from DR and not from MR. Matsuzaki et al. (1993) showed that retrograde tracer injections in SME resulted in dense DR but minimal MR labeling, and DR lesions produced a virtual total loss of 5-HT staining in SME.

Dopamine-containing cell region of the anteromedial zona incerta. MR projects densely to a restricted region of the rostral diencephalon directly ventral to the mammillothalamic tract (Figs. 4, 8; Table 1). This region corresponds to the anteromedial part of the zona incerta (ZIm) or the location of dopamine-containing cells in the medial ZI (A13 DA group) (Dahlstrom and Fuxe, 1964; Bjorklund and Nobin, 1973; Chan-Palay et al., 1984; van den Pol et al., 1984). To our knowledge, no previous report has described MR projections to this site.

Although this DA system (A13) was originally thought mainly to distribute locally to parts of the hypothalamus (an incertohypothalamic system) (Bjorklund et al., 1975), recent evidence indicates that A13 fibers project much more widely; i.e., not only to the hypothalamus but also beyond it to various parts of the limbic forebrain. For instance, recent reports have demonstrated significant ZIm (A13) projections to the central nucleus of the amygdala (CEA), bed nucleus of stria terminalis (BNST), and the horizontal and vertical limbs of the diagonal band nuclei as well as *dopaminergic* ZIm projections to CEA and DBh (Eaton et al., 1994; Wagner et al., 1995). ZIm reportedly regulates gonadotropin secretion (MacKenzie et al., 1984; James et al., 1987), and MR appears to act on ZIm in the release of gonadotropins (Morello and Taleisnik, 1985; Morello et al., 1989).

Basal forebrain and septum. MR fibers distribute heavily to the diagonal band nuclei, and to the medial and lateral septum, and by contrast, minimally to most other structures of the basal forebrain, including the medial and lateral preoptic areas, BNST, the substantia innominata, and the magnocellular preoptic nucleus (Figs. 4, 10, 11; Table 1).

The septum has previously been shown to be a major forebrain target of MR (Segal and Landis, 1974; Bobillier et al., 1979; Azmitia and Segal, 1978; Kohler et al., 1982; Vertes, 1988; Vertes and Martin, 1988). We previously demonstrated (Vertes, 1988) that WGA-HRP injections in MS produced dense cell labeling in MR; the MR was among the most heavily labeled sites in the brainstem.

The MR projection to the septum appears to be predominantly serotonergic. There is a significant overlap in the septum in the distribution of fibers originating from MR and serotonin-containing fibers; that is, 5-HT fibers, like those from MR, are densely concentrated in the MS and lateral LS (Kohler et al., 1982; Gall and Moore, 1984). Combining 5-HT immunochemistry with retrograde tracing, Kohler et al. (1982) demonstrated that approximately 80% of MR cells projecting to the septum stain positively for 5-HT, whereas Crunelli and Segal (1985), by using electrophysiologic techniques, showed that 42% (35 of 83) of MR cells antidromically activated from the MS were serotonergic. 5-HT fibers, putatively of MR origin, form pericellular baskets around cells of the lateral/dorsolateral septum (Kohler et al., 1982; Gall and Moore, 1984; Jakab and Leranth, 1995). 5-HT/5-HT agonists have been shown to inhibit (hyperpolarize) cells of the dorsolateral septum (Joels et al., 1987; Joels and Gallagher, 1988; Van den Hoof

and Galvan, 1992; Gallagher et al., 1995) and inhibit (Segal, 1974, 1986) or excite (Alreja, 1996; Liu and Alreja, 1997) those of the medial septum.

Finally, retrograde examinations of brainstem afferents to various structures of the basal forebrain (Vertes, 1988; Semba et al., 1988; Jones and Cuello, 1989) have, in accord with present results, described large numbers of labeled cells in MR with injections in the septum or diagonal band nuclei, but exceedingly few with injections in the substantia innominata, the magnocellular preoptic nucleus, globus pallidus, ventral pallidum, or olfactory tubercle.

Hippocampal formation. MR fibers distribute heavily throughout the dorsal and ventral HF (Figs. 4, 12–15; Table 1). Previous reports have similarly demonstrated pronounced MR-HF projections (Moore and Halaris, 1975; Azmitia and Segal, 1978; Bobillier et al., 1979; Wyss et al., 1979; Amaral and Cowan, 1980; Riley and Moore, 1981; Kohler and Steinbusch, 1982; Vertes and Martin, 1988), and like here, have shown that MR fibers strongly target the stratum moleculare-lacunosum of CA1 and infragranular zone of DG (Moore and Halaris, 1975; Vertes and Martin, 1988).

The MR projection to HF, like that to the septum, appears to be mainly serotonergic. Combining retrograde tracing with 5-HT immunostaining, Kohler and Steinbusch (1982) reported that the majority of MR cells projecting to HF reacted positively for 5-HT, whereas Moore and Halaris (1975) demonstrated that electrolytic lesions of MR produced a 73% decrease in 5-HT levels in HF. Recent evidence indicates that MR fibers distributing to HF mainly terminate on hippocampal interneurons (Freund et al., 1990; Halasy et al., 1992; Hornung and Celio, 1992).

Serotonin has multiple effects in the hippocampus. 5-HT has been shown to (1) hyperpolarize or depolarize pyramidal cells by actions on 5-HT_{1A} or 5-HT_4 receptors, respectively (Andrade and Nicoll, 1987; Colino and Halliwell, 1987; Chaput et al., 1990; Andrade and Chaput, 1991; Beck, 1992; Beck et al., 1992); (2) hyperpolarize dentate granule cells (Baskys et al., 1989; Piguet and Galvan, 1994); and (3) hyperpolarize/inhibit interneurons (by actions on 5-HT_{1A} receptors) (Schmitz et al., 1995; Bijak and Misgeld, 1997) or depolarize/excite them (primarily by actions on 5-$HT_{3,4}$ receptors) (Kawa, 1994; Bijak and Misgeld, 1997), thereby disinhibiting or inhibiting principal cells, respectively (Segal, 1990; Ropert and Guy, 1991; Oleskevich and Lacaille, 1992; Ghadimi et al., 1994; Schmitz et al., 1995; Siarey et al., 1995; Bijak and Misgeld, 1997).

These diverse actions of 5-HT on cells of the HF suggest a complex functional role(s) for MR/5-HT systems in the hippocampus. In this regard, it has been shown that (1) the application of 5-HT in the hippocampal slice (Ropert, 1988, Klancnik et al., 1989; Richter-Levin and Segal, 1990) or MR stimulation in intact preparations enhances population responses in the HF (Winson, 1980; Srebro et al., 1982; Klancnik and Phillips, 1991; Kao et al., 1997); and (2) MR stimulation desynchronizes the EEG activity of the hippocampus (Vertes, 1981; Vertes and Kocsis, 1997) (see also below).

Cortex. Overall, MR projects lightly to the cortex; that is, lightly to moderately to the entorhinal, perirhinal, and frontal cortices, and sparingly, if at all, to remaining regions of cortex (Fig. 4; Table 1). These findings were unexpected given that the cortex is richly supplied with 5-HT fibers (for review, Jacobs and Azmitia, 1992).

It is well established for several species (Kosofsky and Molliver, 1987; Mulligan and Tork, 1988; Hornung et al., 1990; Voigt and de Lima, 1991) that the cortex contains two major types of 5-HT fibers: (1) thin fibers with small oval or fusiform varicosities, shown to originate from the DR; and (2) thicker fibers with large spherical varicosities, shown to originate from the MR (see Fig. 8, p. 166 from Kosofsky and Molliver, 1987). It has further been demonstrated that DR-type fibers (small varicose) are abundant and widespread in cortex, whereas MR-type fibers are limited and mainly confined to specific regions of cortex, namely, the entorhinal and cingulate cortices (Kosofsky and Molliver, 1987; Mulligan and Tork, 1988; Hornung et al., 1990; Wilson and Molliver, 1991). For instance, Mulligan and Tork (1988) reported for cats that approximately 90% of cortical 5-HT fibers were DR type and only about 10% were MR type fibers. Similar percentages have been described for other species (rats, ferrets, and monkeys) (Kosofsky and Molliver, 1987; Hornung et al., 1990; Voigt and de Lima, 1991; Wilson and Molliver, 1991). These findings are consistent with the present demonstration of limited MR projections to cortex.

Along similar lines, injections of retrograde tracers in various regions of cortex have been shown to give rise to relatively small numbers of labeled cells in MR (i.e., considerably fewer than found in DR) (Kohler and Steinbusch, 1982; Deacon et al., 1983; O'Hearn and Molliver, 1984; Room and Groenewegen, 1986; Waterhouse et al., 1986; Newman and Liu, 1987; Datiche et al., 1995). For example, Waterhouse et al. (1986) identified significant numbers of labeled cells in DR, compared with few in MR, after HRP injections in the motor, sensorimotor, and visual cortices of rats. They stated, "A small number of HRP-filled cells were routinely observed in the MR nucleus after injections in the motor area of cortex. Labeling was very sparse and sometimes absent in the MR after sensorimotor or visual cortical injections."

Although, overall, MR projects lightly to cortex, we demonstrated moderate MR projections to the entorhinal, perirhinal, cingulate, and frontal (motor) cortices. This finding is consistent with the results of previous reports showing moderate numbers of labeled cells in MR after retrograde tracer injections in these cortical regions (Kohler and Steinbusch, 1982; Deacon et al., 1983; O'Hearn and Molliver, 1984; Room and Groenewegen, 1986; Newman and Liu; 1987).

Comparison of projections from the median and dorsal raphe nuclei

A comparison of projections of the median (present results) and dorsal (Vertes, 1991; Vertes and Kocsis, 1994) raphe nuclei (see Fig. 16) shows that the MR and DR distribute to separate, essentially nonoverlapping, sites in the forebrain. As shown here, MR fibers mainly distribute to midline/para-midline structures (Fig. 16A). DR fibers, on the other hand, (Fig. 16B) primarily project laterally to such sites as the substantia nigra pars compacta, amygdala, striatum, BNST, lateral preoptic area, substantia innominata, magnocellular preoptic nucleus, nucleus accumbens, and several regions of cortex (Vertes, 1991). The DR and MR send few projections to common sites (Fig. 16). In the few instances of overlapping projections, it is generally the case that the two nuclei distribute to sepa-

rate parts of a structure/complex. This is best exemplified by projections to the septum (Figs. 10, 11). The MR distributes to medial septum and to the lateral LS but not to the medial LS; by contrast, the DR distributes selectively to the medial LS, avoiding remaining regions of septum (Vertes, 1991). In effect, the raphe/5-HT innervation of the forebrain is shared by MR and DR. These differential projections undoubtedly reflect important functional differences of the two systems.

Role of the MR in the desynchronization of the hippocampal EEG and its functional significance

It is well established that the MR 5-HT system is directly involved in the desynchronization of the hippocampal EEG. For instance, it has been shown that (1) MR stimulation desynchronizes the hippocampal EEG (Macadar et al., 1974; Assaf and Miller, 1978; Yamamoto et al., 1979; Vertes, 1981); (2) MR lesions produce constant theta independent of behavior (Maru et al., 1979; Yamamoto et al., 1979); and (3) injections of various agents into the MR of rats that suppress the activity of 5-HT MR neurons (e.g., 5-HT agonists, excitatory amino acid antagonists, or GABA agonists) produce theta (i.e., block desynchronization) (Vertes et al., 1994; Kinney et al., 1994, 1995). Consistent with the foregoing, Marrosu et al. (1996) recently demonstrated that i.v. injections of 5-HT_{1A} agonists in behaving cats decreased the discharge of midbrain 5-HT cells (through autoreceptor mechanisms) and generated theta (Marrosu et al., 1996).

An accumulating body of evidence indicates that the theta rhythm of the hippocampus is critically involved in memory processing functions of the hippocampus (for review, Vertes, 1986; Vertes and Kocsis, 1997). If, as indicated, theta serves an important role in LTP/memory, it seems to follow that a 5-HT MR mediated disruption of theta (hippocampal desynchronization) might suppress LTP and memory. Consistent with this possibility, several reports have shown that serotonergic agents block LTP and that 5-HT antagonists (mainly 5-HT_3 antagonists) enhance LTP, memory, or both (Corradetti et al., 1992; Staubli and Otaky, 1994; Staubli and Xu, 1995; Buhot, 1997; Vertes and Kocsis, 1997).

The foregoing suggests that ascending 5-HT MR systems, by disrupting theta (or desynchronizing the hippocampal EEG), may block or temporarily suspend mnemonic processes in the hippocampus. Memory obviously favors significant over nonsignificant events. The MR may be an important part of a system of connections that directs the hippocampus to essentially disregard insignificant environmental events.

In summary, the MR projects widely to structures of the brainstem and forebrain and undoubtedly exerts a significant modulatory influence on these structures, especially on the septum-hippocampus in the control of hippocampal EEG activity and possibly mnemonic functions of the hippocampus.

ACKNOWLEDGMENTS

We thank Nedialka Todorova for superb technical assistance and Sherri Von Hartman for excellent graphic work. WJF was supported in part by predoctoral fellowships from the Newell Foundation of Florida Atlantic University and from the Bryan W. Robinson Neurological Foundation.

LITERATURE CITED

Aghajanian GK, Wang RY. 1977. Habenular and other midbrain raphe afferents demonstrated by a modified retrograde tracing technique. Brain Res 122:229–242.

Allen GV, Hopkins DA. 1989. Mammillary body in the rat: topography and synaptology of projections from the subicular complex, prefrontal cortex, and midbrain tegmentum. J Comp Neurol 286:311–336.

Alreja M. 1996. Excitatory actions of serotonin on GABAergic neurons of the medial septum and diagonal band of Broca. Synapse 22:15–27.

Amaral DG, Cowan WM. 1980. Subcortical afferents to the hippocampal formation in the monkey. J Comp Neurol 189:573–591.

Andrade R, Chaput Y. 1991. 5-hydroxytryptamine-like receptors mediate slow excitatory responses to serotonin in the rat hippocampus. J Pharmacol Exp Ther 257:930–937.

Andrade R, Nicoll RA. 1987. Pharmacologically distinct actions of serotonin on single pyramidal neurones of the rat hippocampus recorded in vitro. J Physiol. (Lond) 394:99–124.

Araki M, McGeer PL, Kimura H. 1988. The efferent projections of the rat lateral habenular nucleus revealed by the PHA-L anterograde tracing method. Brain Res 441:319–330.

Assaf SY, Miller JJ. 1978. The role of a raphe serotonin system in the control of septal unit activity and hippocampal desynchronization. Neuroscience 3:539–550.

Azmitia EC, Segal M. 1978. An autoradiographic analysis of the differential ascending projections of the dorsal and median raphe nuclei in the rat. J Comp Neurol 179:641–668.

Baskys A, Niesen CE, Davies MF, Carlen PL. 1989. Modulatory actions of serotonin on ionic conductances of hippocampal dentate granule cells. Neuroscience 29:443–451.

Bayev KV, Beresovskii VK, Kebkalo TG, Savoskina LA. 1988. Afferent and efferent connections of brainstem locomotor regions: study by means of horseradish peroxidase transport technique. Neuroscience 26:871–891.

Beck SG. 1992. 5-hydroxytryptamine increases excitability of CA1 hippocampal pyramidal cells. Synapse 10:334–340.

Beck SG, Choi KC, List TJ. 1992. Comparison of 5-hydroxytryptamine$_{1A}$ mediated hyperpolarization in CA1 and CA3 hippocampal pyramidal cells. J Pharmacol Exp Ther 263:350–359.

Behzadi G, Kalen P, Parvopassu F, Wiklund L. 1990. Afferents to the median raphe nucleus of the rat: retrograde cholera toxin and wheat germ conjugated horseradish peroxidase tracing, and selective D-[^{3}H]aspartate labelling of possible excitatory amino acid inputs. Neuroscience 37:77–100.

Beitz AJ. 1982. The organization of afferent projections to the midbrain periaqueductal gray of the rat. Neuroscience 7:133–159.

Beitz AJ, Clements JR, Mullett MA, Ecklund LJ. 1986. Differential origin of brainstem serotoninergic projections to the midbrain periaqueductal gray and superior colliculus of the rat. J Comp Neurol 250:498–509.

Bijak M, Misgeld U. 1997. Effects of serotonin through serotonin$_{1A}$ and serotonin4 receptors on inhibition in the guinea-pig dentate gyrus in vitro. Neuroscience 78:1017–1026.

Bjorklund A, Nobin A. 1973. Fluorescence histochemical and microspectrofluorometric mapping of dopamine and noradrenaline cell groups in the rat diencephalon. Brain Res 51:193–205.

Bjorklund A, Lindvall O, Nobin A. 1975. Evidence of an incertohypothalamic dopamine neurone system in the rat. Brain Res 89:29–42.

Bobillier P, Petitjean F, Salvert D, Ligier M, Seguin S. 1975. Differential projections of the nucleus raphe dorsalis and nucleus raphe centralis as revealed by autoradiography. Brain Res 85:205–210.

Bobillier P, Seguin S, Petitjean F, Salvert D, Touret M, Jouvet M. 1976. The raphe nuclei of the cat brain stem: a topographical atlas of their efferent projections as revealed by autoradiography. Brain Res 113:449–486.

Bobillier P, Seguin S, Degueurce A, Lewis BD, Pujol JF. 1979. The efferent connections of the nucleus centralis superior in the rat as revealed by autoradiography. Brain Res 113:449–486.

Buhot M-C. 1997. Serotonin receptors in cognitive behaviors. Curr Opin Neurobiol 7:243–254.

Carstens E, Leah J, Lechner J, Zimmermann M. 1990. Demonstration of extensive brainstem projections to medial and lateral thalamus and hypothalamus in the rat. Neuroscience 35:609–626.

Chan-Palay V, Zaborsky K, Kohler C, Goldstein M, Palay SL. 1984. Distribution of tyrosine-hydroxylase immunoreactive neurons in the hypothalamus of rats. J Comp Neurol 227:467–496.

Chaput Y, Araneda RC, Andrade R. 1990. Pharmacological and functional analysis of a novel serotonin receptor in the rat hippocampus. Eur J Pharmacol 182:441–456.

Chen S, Su H-S. 1990. Afferent connections of the thalamic paraventricular and paratenial nuclei in the rat: a retrograde tracing study with iontophoretic application of Fluoro-Gold. Brain Res 522:1–6.

Clements JR, Beitz AJ, Fletcher TF, Mullett MA. 1985. Immunocytochemical localization of serotonin in the rat periaqueductal gray: a quantitative light and electron microscopic study. J Comp Neurol 236:60–70.

Coffield JA, Bowen KK, Miletic V. 1992. Retrograde tracing of projections between the nucleus submedius, the ventrolateral orbital cortex, and the midbrain in the rat. J Comp Neurol 321:488–499.

Colino A, Halliwell JV. 1987. Differential modulation of three separate K^+ conductances in hippocampal CA1 neurons by serotonin. Nature 328: 73–77.

Comans PE, Snow PJ. 1981. Ascending projections to nucleus parafascicularis of the cat. Brain Res 230:337–341.

Conrad LCA, Leonard CM, Pfaff DW. 1974. Connections of the median and dorsal raphe nuclei in the rat: an autoradiographic and degeneration study. J Comp Neurol 156:179–206.

Contestabile A, Flumerfelt BA. 1981. Afferent connections of the interpeduncular nucleus and the topographic organization of the habenulo-interpeduncular pathway: an HRP study in the rat. J Comp Neurol 196:253–270.

Cornwall J, Phillipson OT. 1988a. Afferent projections to the dorsal thalamus of the rat as shown by retrograde lectin transport: I. The mediodorsal nucleus. Neuroscience 24:1035–1049.

Cornwall J, Phillipson OT. 1988b. Afferent projections to the dorsal thalamus of the rat as shown by retrograde lectin transport: II. The midline nuclei. Brain Res Bull 21:147–161.

Cornwall J, Cooper JD, Phillipson OT. 1990. Afferent and efferent connections of the laterodorsal tegmental nucleus in the rat. Brain Res Bull 25:271–284.

Corradetti R, Ballerini L, Pugliese AM, Pepeu G. 1992. Serotonin blocks the long-term potentiation induced by primed burst stimulation in the CA1 region of rat hippocampal slices. Neuroscience 46:511–518.

Craig AD, Burton H. 1981. Spinal and medullary lamina I projection to nucleus submedius in medial thalamus: a possible pain center. J Neurophysiol 45:443–466.

Crunelli V, Segal M. 1985. An electrophysiological study of neurones in the rat median raphe and their projections to the septum and hippocampus. Neuroscience 15:47–60.

Dahlstrom A, Fuxe K. 1964. Evidence for the existence of monoamine-containing neurons in the central nervous system: I. Demonstration of monoamines in the cell bodies of brainstem neurons. Acta Physiol Scand Suppl 232, 62:1–55.

Datiche F, Luppi P-H, Cattarelli M. 1995. Serotonergic and non-serotonergic projections from the raphe nuclei to the piriform cortex in the rat: a cholera toxin B subunit (CTb) and 5-HT immunohistochemical study. Brain Res 671:27–37.

Datta S. 1995. Neuronal activity in the peribrachial area: relationship to behavioral state control. Neurosci Biobehav Rev 19:67–84.

Deacon TW, Eichenbaum H, Rosenberg P, Eckmann KW. 1983. Afferent connections of the perirhinal cortex in the rat. J Comp Neurol 220:168–190.

Eaton MJ, Wagner CK, Moore KE, Lookingland KJ. 1994. Neurochemical identification of A_{13} dopaminergic neuronal projections from the medial zona incerta to the horizontal limb of the diagonal band of Broca and the central nucleus of the amygdala. Brain Res 659:201–207.

Freund TF, Gulyas AI, Acsadi L, Gorcs T, Toth K. 1990. Serotonergic control of the hippocampus via local inhibitory interneurons. Proc Natl Acad Sci USA 87:8501–8505.

Gall C, Moore RY. 1984. Distribution of enkaphalin, substance P, tyrosine hydroxylase, and 5-hydroxytryptamine immunoreactivity in the septal region of the rat. J Comp Neurol 225:212–227.

Gallager DW, Pert G. 1978. Afferents to brain stem nuclei (brain stem raphe, nucleus reticularis pontis caudalis and nucleus gigantocellularis) in the rat as demonstrated by microiontophoretically applied horseradish peroxidase. Brain Res 144:257–275.

Gallagher JP, Zheng F, Hasuo H, Shinnick-Gallagher P. 1995. Activities of neurons within the rat dorsolateral septal nucleus (DLSN) Prog Neurbiol 45:373–395.

Geeraedts LMG, Nieuwenhuys R, Veening JG. 1990a. Medial forebrain bundle of the rat: III. Cytoarchitecture of the rostral (telencephalic) part of the medial forebrain bundle bed nucleus. J Comp Neurol 294:507–536.

Geeraedts LMG, Nieuwenhuys R, Veening JG. 1990b. Medial forebrain bundle of the rat: IV. Cytoarchitecture of the caudal (lateral hypothalamic) part of the medial forebrain bundle bed nucleus. J Comp Neurol 294:537–568.

Gerfen CR, Sawchenko PE. 1984. An anterograde neuroanatomical tracing method that shows the detailed morphology of neurons, their axons and terminals: immunohistochemical localization of an axonally transported plant lectin, *Phaseolus vulgaris* leucoagglutinin (PHA-L). Brain Res 290:219–238.

Ghadimi BM, Jarolimek W, Misgeld U. 1994. Effects of serotonin on hilar neurons and granule cell inhibition in the guinea pig hippocampal slice. Brain Res 633:27–32.

Groenewegen HJ. 1988. Organization of the afferent connections of the mediodorsal thalamic nucleus in the rat, related to the mediodorsal-prefrontal topography. Neuroscience 24:379–431.

Groenewegen HJ, Ahlenius S, Haber SN, Kowall NW, Nauta WJH. 1986. Cytoarchitecture, fiber connections, and some histochemical aspects of the interpeduncular nucleus of the rat. J Comp Neurol 249:65–102.

Halasy K, Miettinen R, Szabat E, Freund TF. 1992. GABAergic interneurons are the major postsynaptic targets of median raphe afferents in the rat dentate gyrus. Eur J Neurosci 4:144–153.

Halliday G, Harding A, Paxinos G. 1995. Serotonin and tachykinin systems. In: Paxinos G, editor. The rat nervous system, 2nd ed. New York: Academic Press. p 929–974.

Hamill GS, Jacobowitz DM. 1984. A study of afferent projections to the rat interpeduncular nucleus. Brain Res Bull 13:527–539.

Hamill GS, Olschowka JA, Lenn NJ, Jacobowitz DM. 1984. The subnuclear distribution of substance P, cholecystokinin, vasoactive intestinal peptide, somatostatin, leu-enkephalin, dopamine-β-hydroxylase, and serotonin in the rat interpeduncular nucleus. J Comp Neurol 226:580–596.

Hayakawa T, Zyo K. 1984. Comparative anatomical study of the tegmento-mammillary projections in some mammals: a horseradish peroxidase study. Brain Res 300:335–349.

Hayakawa T, Ito H, Zyo K. 1993. Neuroanatomical study of afferent projections to the supramammillary nucleus in the rat. Anat Embryol 188:139–148.

Herkenham M. 1978. The connections of the nucleus reuniens thalami: evidence for a direct thalamo-hippocampal pathway in the rat. J Comp Neurol 177:589–610.

Herkenham M. 1979. The afferent and efferent connections of the ventromedial thalamic nucleus in the rat. J Comp Neurol 183:487–518.

Herkenham M, Nauta WJH. 1977. Afferent connections of the habenular nuclei in the rat: a horseradish peroxidase study, with a note on the fiber-of-passage problem. J Comp Neurol 173:123–146.

Herkenham M, Nauta WJH. 1979. Efferent connections of the habenular nuclei in the rat. J Comp Neurol 187:19–248.

Hornung J-P, Celio MR. 1992. The selective innervation by serotonergic axons of calbindin-containing interneurons in the neocortex and hippocampus of the marmoset. J Comp Neurol 320:457–467.

Hornung J-P, Fritschy J-M, Tork I. 1990. Distribution of two morphologically distinct subsets of serotonergic axons in the cerebral cortex of the marmoset. J Comp Neurol 297:165–181.

Jacobs BL, Azmitia EC. 1992. Structure and function of the brain serotonin system. Physiol Rev 72:165–229.

Jakab RL, Leranth C. 1995. Septum. In: Paxinos G, editor. The rat nervous system, 2nd ed. New York: Academic Press. p 405–422.

James MD, MacKenzie FJ, Tuohy-Jones PA, Wilson CA. 1987. Dopaminergic neurones in the zona incerta exert a stimulatory control on gonadotrophin release via D_1 dopamine receptors. Neuroendocrinology 43:348–355.

Jimenez-Castellanos J, Reinoso-Suarez F. 1985. Topographical organization of the afferent connections of the principal ventromedial thalamic nucleus in the cat. J Comp Neurol 236:297–314.

Joels M, Gallagher JP. 1988. Actions of serotonin recorded intracellularly in rat dorsal lateral septal neurons. Synapse 2:45–53.

Joels M, Shinnick-Gallagher P, Gallagher JP. 1987. Effect of serotonin and serotonin-analogues on passive membrane properties of lateral septal neurons in vitro. Brain Res 417:99–107.

Jones BE. 1991. Paradoxical sleep and its chemical/structural substrates in the brain. Neuroscience 40:637–656.

Jones BE, Cuello AC. 1989. Afferents to the basal forebrain cholinergic cell area from pontomesencephalic—catecholamine, serotonin, and acetylcholine – neurons. Neuroscience 31:37–61.

Kalen P, Skagerberg G, Lindvall O. 1988. Projections from the ventral tegmental area and mesencephalic raphe to the dorsal raphe nucleus in the rat. Exp Brain Res 73:69–77.

Kao K, Sanders MJ, Green EJ. 1997. Physiological evidence for hippocampal disinhibition resulting from activation of the median raphe. Brain Res 752:90–98.

Kawa K. 1994. Distribution and functional properties of 5-HT_3 receptors in the rat dentate gyrus: a patch-clamp study. J Neurophysiol 71:1935–1947.

Kinney GG, Kocsis B, Vertes RP. 1994. Injections of excitatory amino acid antagonists into the median raphe nucleus produce hippocampal theta rhythm in the urethane anesthetized rat. Brain Res 654:96–104.

Kinney GG, Kocsis B, Vertes RP. 1995. Injections of muscimol into the median raphe nucleus produce hippocampal theta rhythm in the rat. Psychopharmacology 120:244–248.

Klancnik JM, Phillips AG. 1991. Modulation of synaptic plasticity in the dentate gyrus of the rat by electrical stimulation of the median raphe nucleus. Brain Res 557:236–240.

Klancnik JM, Baimbridge KG, Phillips AG. 1989. Increased population spike amplitude in the dentate gyrus following systemic administration of 5-hydroxytryptophan or 8-hydroxy-2-(di-n-propylamino)-tetralin. Brain Res 505:145–148.

Kobayashi Y, Matsuyama K, Mori S. 1994. Distribution of serotonin cells projecting to the pontomedullary reticular formation in the rat. Neurosci Res 20:43–55.

Kohler C, Steinbusch H. 1982. Identification of serotonin and nonserotonin-containing neurons of the mid-brain raphe projecting to the entorhinal area and the hippocampal formation. A combined immunohistochemical and fluorescent retrograde tracing study in the rat. Neuroscience 7:951–975.

Kohler C, Chan-Palay V, Steinbusch H. 1982. The distribution and origin of serotonin-containing fibers in the septal area: a combined immunohistochemical and fluorescent retrograde tracing study in the rat. J Comp Neurol 209:91–111.

Kosofsky BE, Molliver ME. 1987. The serotonergic innervation of cerebral cortex: different classes of axon terminals arise from the dorsal and median raphe nuclei. Synapse 1:153–168.

Larsen KD, McBride RL. 1979. The organization of the feline entopeduncular nucleus projections: anatomical studies. J Comp Neurol 184:293–308.

Leonard CS, Llinas R. 1990. Electrophysiology of pedunculopontine and laterodorsal tegmental neurons in vitro: implications for the control of REM sleep. In: Steriade M, Biesold D, editors. Brain cholinergic systems. New York: Oxford University Press, p. 205–223.

Liu W, Alreja M. 1997. Atypical antipsychotics block the excitatory effects of serotonin in septohippocampal neurons in the rat. Neuroscience 79:369–382.

Macadar AW, Chalupa LM, Lindsley DB. 1974. Differentiation of brain stem loci which affect hippocampal and neocortical electrical activity. Exp Neurol 43:499–514.

Maciewicz R, Foote WE, Bry J. 1981. Excitatory projection from the interpeduncular nucleus to central superior raphe neurons. Brain Res 225:179–183.

MacKenzie FJ, Hunter AJ, Daly C, Wilson CA. 1984. Evidence that the dopaminergic incerto-hypothalamic tract has a stimulatory effect on ovulation and gonadotrophin release. Neuroendocrinology 39:289–295.

Marchand ER, Riley JN, Moore RY. 1980. Interpeduncular nucleus afferents in the rat. Brain Res 193:339–352.

Marcinkiewicz M, Morcos R, Chretien M. 1989. CNS connections with the median raphe nucleus: retrograde tracing with WGA-apoHRP-gold complex in the rat. J Comp Neurol 289:11–35.

Marrosu F, Fornal CA, Metzler CW, Jacobs BL. 1996. 5-HT1A agonists induce hippocampal theta activity in freely moving rats: role of presynaptic 5-HT1A receptors. Brain Res 739:192–200.

Maru E, Takahashi LK, Iwahara S. 1979. Effects of median raphe nucleus lesions on hippocampal EEG in the freely moving rat. Brain Res 163:223–234.

Matsuzaki S, Takada M, Li Y-Q, Tokuno H, Mizuno N. 1993. Serotonergic projections from the dorsal raphe nucleus to the nucleus submedius in the rat and cat. Neuroscience 55:403–416.

McGuinness CM, Krauthamer GM. 1980. The afferent projections of the centrum medianum of the cat as demonstrated by retrograde transport of horseradish peroxidase. Brain Res 184:255–269.

Meller ST, Dennis BJ. 1986. Afferent projections to the periaqueductal gray in the rabbit. Neuroscience 19:927–964.

Moore RY, Halaris AE. 1975. Hippocampal innervation by serotonin neurons of the midbrain raphe in the rat. J Comp Neurol 164:171–184.

Moore RY, Halaris AE, Jones BE. 1978. Serotonin neurons of the midbrain raphe: ascending projections. J Comp Neurol 180:417–438.

Morello H, Taleisnik S. 1985. Changes in the release of luteinizing hormone (LH) on the day of proestrous after lesions or stimulation of the raphe nuclei in rats. Brain Res 360:311–317.

Morello H, Caligaris L, Haymal B, Taleisnik S. 1989. Inhibition of proestrous LH surge and ovulation in rats evoked by stimulation of the median raphe nucleus involves a GABA-mediated mechanism. Neuroendocrinology 50:81–87.

Mulligan KA, Tork I. 1988. Serotonergic innervation of the cat cerebral cortex. J Comp Neurol 270:86–110.

Nakano K, Kohno M, Hasegawa Y, Tokushige A. 1985. Cortical and brain stem afferents to the ventral thalamic nuclei of the cat demonstrated by retrograde axonal transport of horseradish peroxidase. J Comp Neurol 231:102–120.

Nauta WJH. 1958. Hippocampal projections and related neural pathways to the mid-brain in the cat. Brain 81:319–341.

Nauta WJH. 1974. Evidence of a pallidohabenular pathway in the cat. J Comp Neurol 156:19–28.

Newman DB, Ginsberg CY. 1994. Brainstem reticular nuclei that project to the thalamus in rats: a retrograde tracer study. Brain Behav Evol 44:1–39.

Newman DB, Liu RPC. 1987. Nuclear origins of brainstem reticulocortical systems in the rat. Am J Anat 178:279–299.

Nieuwenhuys R, Geeraedts LMG, Veening JG. 1982. The medial forebrain bundle of the rat. I. General introduction. J Comp Neurol 206:49–81.

O'Hearn E, Molliver ME. 1984. Organization of raphe-cortical projections in rat: a quantitative retrograde study. Brain Res Bull 13:709–726.

Oleskevich S, Lacaille JC. 1992. Reduction of $GABA_B$ inhibitory postsynaptic potentials by serotonin via presynaptic and postsynaptic mechanisms in CA3 pyramidal cells of rat hippocampus in vitro. Synapse 12:173–188.

Parent A, Descarries L, Beaudet A. 1981. Organization of ascending serotonin systems in the adult rat brain: a radioautographic study after intraventricular administration of [^{3}H] 5-hydroxytryptamine. Neuroscience 6:115–138.

Paxinos G, Watson C. 1986. The rat brain in stereotaxic coordinates, 2nd ed. New York: Academic Press.

Peschanski M, Besson J-M. 1984. Diencephalic connections of the raphe nuclei of the rat brainstem: an anatomical study with reference to the somatosensory system. J Comp Neurol 224:509–534.

Piguet P, Galvan M. 1994. Transient and long-lasting actions of 5-HT on rat dentate gyrus neurones in vitro. J Physiol (Lond) 481:629–639.

Rasmussen K, Heym J, Jacobs BL. 1984. Activity of serotonin-containing neurons in nucleus centralis superior of freely moving cats. Exp Neurol 83: 302–317.

Richter-Levin G, Segal M. 1990. Effect of serotonin releasers on dentate granule cell excitability in the rat. Exp Brain Res 82:199–207.

Riley JN, Moore RY. 1981. Diencephalic and brainstem afferents to the hippocampal formation of the rat. Brain Res Bull 6:437–444.

Room P, Groenewegen HJ. 1986. Connections of the parahippocampal cortex in the cat: II. Subcortical afferents. J Comp Neurol 251:451–473.

Ropert N. 1988. Inhibitory action of serotonin in CA1 pyramidal neurons in vitro. Neuroscience 36:631–641.

Ropert N, Guy N. 1991. Serotonin facilitates GABAergic transmission in the CA1 region of rat hippocampus in vitro. J Physiol (Lond) 441:121–136.

Royce GJ, Bromley S, Gracco C. 1991. Subcortical projections to the centromedian and parafascicular thalamic nuclei in the cat. J Comp Neurol 306:129–155.

Sakai K, Salvert D, Touret M, Jouvet M. 1977. Afferent connections of the nucleus raphe dorsalis in the cat as visualized by the horseradish peroxidase technique. Brain Res 137:11–35.

Schmitz D, Empson RM, Heinemann U. 1995. Serotonin reduces inhibition via 5-HT_{1A} receptors in area CA1 of rat hippocampal slices in vitro. J Neurosci 15:7217–7225.

Segal M. 1974. Responses of septal nuclei neurons to microiontophoretically administered putative neurotransmitters. Life Sci 14:1345–1351.

Segal M. 1986. Properties of rat medial septal neurons recorded in vitro. J Physiol (Lond) 379:309–330.

Segal M. 1990. Serotonin attenuates a slow inhibitory postsynaptic potential in rat hippocampal neurons. Neuroscience 36:631–641.

Segal M, Landis SC. 1974. Afferents to the septal area of the rat studied with the method of retrograde axonal transport of horseradish peroxidase. Brain Res 82:263–268.

Semba K. 1993. Aminergic and cholinergic afferents to REM sleep induction regions of the pontine reticular formation in the rat. J Comp Neurol 330:543–556.

Semba K, Fibiger HC. 1992. Afferent connections of the laterodorsal and the pedunculopontine tegmental nuclei in the rat: a retro- and anterograde transport and immunohistochemical study. J Comp Neurol 323:387–410.

Semba K, Reiner PB, McGeer EG, Fibiger HC. 1988. Brainstem afferents to the magnocellular basal forebrain studied by axonal transport, immunohistochemistry, and electrophysiology in the rat. J Comp Neurol 267:433–453.

Shammah-Lagnado SJ, Ricardo JA, Sakamoto NTMN, Negrao N. 1983. Afferent connections of the mesencephalic reticular formation: a horseradish peroxidase study in the rat. Neuroscience 9:391–409.

Shammah-Lagnado SJ, Negrao N, Silva BA, Ricardo JA. 1987. Afferent connections of the nuclei reticularis pontis oralis and caudalis: a horseradish peroxidase study in the rat. Neuroscience 20:961–989.

Shibata H. 1987. Ascending projections to the mammillary nuclei in the rat: a study using retrograde and anterograde transport of wheat germ agglutinin conjugated to horseradish peroxidase. J Comp Neurol 264: 205–215.

Shibata H, Suzuki T. 1984. Efferent projections of the interpeduncular complex in the rat, with special reference to its subnuclei: a retrograde horseradish peroxidase study. Brain Res 296:345–349.

Shibata H, Suzuki T, Matsushita M. 1986. Afferent projections to the interpeduncular nucleus in the rat, as studied by retrograde and anterograde transport of wheat germ agglutinin conjugated to horseradish peroxidase. J Comp Neurol 248:272–284.

Siarey RJ, Andreasen M, Lambert JDC. 1995. Serotonergic modulation of excitability in area CA1 of the in vitro rat hippocampus. Neurosci Lett 199:211–214.

Srebro B, Azmitia EC, Winson J. 1982. Effect of 5-HT depletion of the hippocampus on neuronal transmission from perforant path through dentate gyrus. Brain Res 235:142–147.

Staubli U, Otaky N. 1994. Serotonin controls the magnitude of LTP induced by theta bursts via an action on NMDA-receptor-mediated responses. Brain Res 643:10–16.

Staubli U, Xu F. 1995. Effects of 5-HT_3 receptor antagonism on hippocampal theta rhythm, memory, and LTP induction in the freely moving rat. J Neurosci 15:2445–2452.

Steinbusch HWM. 1981. Distribution of serotonin-immunoreactivity in the central nervous system of the rat: cell bodies and terminals. Neuroscience 6:557–618.

Steinbusch HWM, Nieuwenhuys R. 1983. The raphe nuclei of the rat brainstem: a cytoarchitectonic and immunohistochemical study. In: Emson PC, editor. Chemical neuroanatomy. New York: Raven Press. p 131–207.

Steininger TL, Rye DB, Wainer BH. 1992. Afferent projections to the cholinergic pedunculopontine tegmental nucleus and adjacent midbrain extrapyramidal area in the albino rat. I. Retrograde tracing studies. J Comp Neurol 321:515–543.

Steininger TL, Rye DB, Wainer BH. 1997. Serotonergic dorsal raphe nucleus projections to the cholinergic and noncholinergic neurons of the pedunculopontine tegmental region: a light and electron microscopic anterograde tracing and immunohistochemical study. J Comp Neurol 382:302–322.

Sutherland RJ. 1982. The dorsal diencephalic conduction system: a review of the anatomy and functions of the habenular complex. Neurosci Biobehav Rev 6:1–13.

Ter Horst GJ, Groenewegen HJ, Karst H, Luiten PGM. 1984. *Phaseolus vulgaris* leuco-agglutinin immunohistochemistry. A comparison between autoradiographic and lectin tracing of neuronal efferents. Brain Res 307:379–383.

Tork I. 1985. Raphe nuclei and serotonin-containing systems. In: Paxinos G, editor. The rat nervous system, Vol 2, Hindbrain and spinal cord. Sydney: Academic Press. p 43–78.

Van den Hoof P, Galvan M. 1992. Actions of 5-hydroxytryptamine and 5-HT_{1A} receptor ligands on rat dorso-lateral septal neurones in vitro. Br J Pharmacol 106:893–899.

van den Pol AN, Herbst RS, Powell JF. 1984. Tyrosine hydroxylase-immunoreactive neurons of the hypothalamus: a light and electron microscopic study. Neuroscience 13:1117–1156.

Veening JG, Swanson LW, Cowan WM, Nieuwenhuys R, Geeraedts LMG. 1982. The medial forebrain bundle of the rat: II. An autoradiographic study of the topography of the major ascending and descending components. J Comp Neurol 206:82–108.

Velayos JL, Reinoso-Suarez F. 1982. Topographic organization of the brainstem afferents to the mediodorsal thalamic nucleus. J Comp Neurol 206:17–27.

Vertes RP. 1981. An analysis of ascending brain stem systems involved in hippocampal synchronization and desynchronization. J Neurophysiol 46:1140–1159.

Vertes RP. 1984. A lectin horseradish peroxidase study of the origin of ascending fibers in the medial forebrain bundle of the rat: the upper brainstem. Neuroscience 11:669–690.

Vertes RP. 1986. Brainstem modulation of the hippocampus: anatomy, physiology and significance. In: Isaacson RL, Pribram KH, editors. The hippocampus, Vol 4. New York: Plenum Press. p 41–75.

Vertes RP. 1988. Brainstem afferents to the basal forebrain in the rat. Neuroscience 24:907–935.

Vertes RP. 1990. Brainstem mechanisms of slow-wave sleep and REM sleep. In: Klemm WR, Vertes RP, editors. Brainstem mechanisms of behavior. New York: John Wiley and Sons. p 535–581.

Vertes RP. 1991. A PHA-L analysis of ascending projections of the dorsal raphe nucleus in the rat. J Comp Neurol 313:643–668.

Vertes RP, Crane AM. 1997. Distribution, quantification and morphological characteristics of serotonin-immunoreactive cells of the supralemniscal nucleus (B9) and pontomesencephalic reticular formation in the rat. J Comp Neurol 378:411–424.

Vertes RP, Kocsis B. 1994. Projections of the dorsal raphe nucleus to the brainstem: PHA-L analysis in the rat. J Comp Neurol 340:11–26.

Vertes RP, Kocsis B. 1997. Brainstem-diencephalo-septohippocampal systems controlling the theta rhythm of the hippocampus. Neuroscience 81:893–926.

Vertes RP, Martin GF. 1988. An autoradiographic analysis of ascending projections from the pontine and mesencephalic reticular formation and the median raphe nucleus in the rat. J Comp Neurol 275:511–541.

Vertes RP, Kinney GG, Kocsis B, Fortin WJ. 1994. Pharmacological suppression of the median raphe nucleus with serotonin$_{1A}$ agonists, 8-OH-DPAT and buspirone, produces hippocampal theta rhythm in the rat. Neuroscience 60:441–451.

Voigt T, de Lima AD. 1991. Serotonergic innervation of the ferret cerebral cortex: I. Adult pattern. J Comp Neurol 314:403–414.

Wagner CK, Eaton MJ, Moore KE, Lookingland KJ. 1995. Efferent projections from the region of the medial zona incerta containing A_{13} dopaminergic neurons: a PHA-L anterograde tract-tracing study in the rat. Brain Res 677:229–237.

Wang RY, Aghajanian GK. 1977. Physiological evidence for habenula as major link between forebrain and midbrain raphe. Science 197:89–91.

Waterhouse BD, Mihailoff GA, Baack JC, Woodward DJ. 1986. Topographical distribution of dorsal and median raphe neurons projecting to motor, sensorimotor, and visual cortical areas in the rat. J Comp Neurol 249:460–476.

Wilson MA, Molliver ME. 1991. The organization of serotonergic projections to cerebral cortex in primates: regional distribution of axon terminals. Neuroscience 44:537–553.

Winson J. 1980. Influence of raphe nuclei on neuronal transmission from perforant pathway through dentate gyrus. J Neurophysiol 44:937–950.

Wyss JM, Swanson LW, Cowan WM. 1979. A study of subcortical afferents to the hippocampal formation in the rat. Neuroscience 4:463–476.

Yamamoto T, Watanabe S, Oishi R, Ueki S. 1979. Effects of midbrain raphe stimulation and lesion on EEG activity in rats. Brain Res Bull 4:491–495.

Yoshida A, Dostrovsky JO, Chiang CY. 1992. The afferent and efferent connections of the nucleus submedius in the rat. J Comp Neurol 324:115–133.